The Unified Theory of Physics

Ding-Yu Chung[1]
P.O. Box 180661, Utica, Michigan 48318, USA

The unified theory of physics unifies various phenomena in our observable universe and other universes. The unified theory is based on the zero-energy universe and the space-object structures. Different universes in different developmental stages are the different expressions of the space-object structures. The unified theory is divided into five parts: the space-object structures, cosmology, the periodic table of elementary particles, the galaxy formation, and the extreme force field. The space-object structures explain quantum mechanics, relativity, and the evolution of the universes. From the zero-energy universe, our universe starts with the 11D (dimensional) membrane dual universe followed by the 10D string dual universe and then by the 10D particle dual universe, and ends with the asymmetrical light-dark dual universe. This 4-stage process goes on in repetitive cycles. Such 4-stage cosmology accounts for the origins of the four force fields. The theoretical calculated percentages of dark energy, dark matter, and baryonic matter are 72.8. 22.7, and 4.53, respectively, in agreement with observed value. According to the calculation, dark energy started in 4.47 billion years ago in agreement with the observed 4.71 ± 0.98 billion years ago. The unified theory places all elementary particles in the periodic table of elementary particles with the calculated masses in good agreement with the observed values, including the mass of the Higgs boson. It explains the inflation, the Big Bang, and the formation of various shapes of galaxies. It gives the structure for the extreme force fields, including superconductivity, black hole, and supernova.

---

[1] electronic mail address: dy_chung@yahoo.com

Contents

1. The Space-Object Structures

The Space Structure

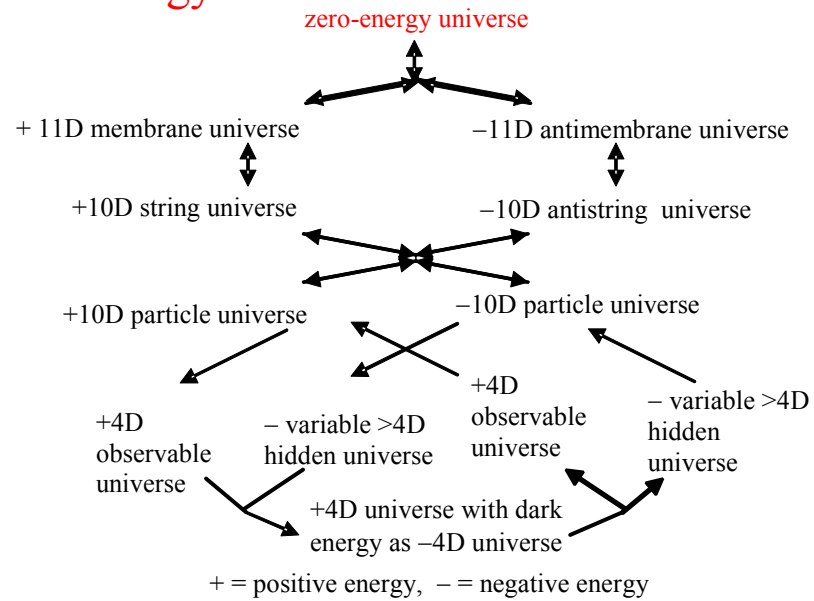$$(1)_n \quad \xleftrightarrow{\text{Higgs Bosons}} \quad (0)_n$$

$$(1)_n + (0)_n \quad \xrightarrow{\text{combination}}$$

$$(1\ 0)_n, \ (1+0)_n, \ \text{or} \ (1)_n(0)_n$$

The Object Structure

$$3_{11}, \ 2_{10}, \ 1_{4 \ to \ 10}, \ 0_{4 \ to \ 11}$$

$$E = M c^2 / \alpha^{2(D-4)}$$

2. Cosmology
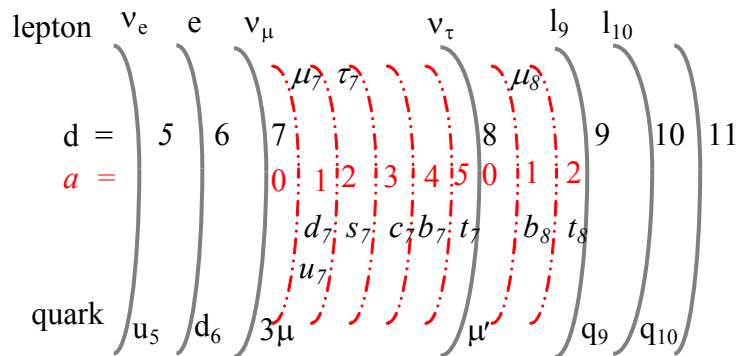
zero-energy universe

+ 11D membrane universe   −11D antimembrane universe

+10D string universe   −10D antistring universe

+10D particle universe   −10D particle universe

+4D observable universe   − variable >4D hidden universe   +4D observable universe   − variable >4D hidden universe

+4D universe with dark energy as −4D universe

+ = positive energy, − = negative energy

3. The Periodic Table of Elementary Particles

lepton ν_e e ν_μ ν_τ l_9 l_{10}

μ_7, τ_7 μ_8

$d =$ 5   6   7   8   9   10   11

$a =$ 0   1   2   3   4   5   0   1   2

$d_7\ s_7\ c_7\ b_7\ t_7$ $b_8\ t_8$

u_7

quark u_5 d_6 3μ μ' q_9 q_{10}

The LHC Higgs Boson

H (hidden lepton condensate) $\longrightarrow$ γ γ

H (SM) $\longrightarrow$ γ γ

H (SM) $\longrightarrow$ Z Z

H (SM) $\longrightarrow$ W W

H (SM) $\longrightarrow$ b $\bar{\text{b}}$

H (SM) $\longrightarrow$ τ $\bar{\tau}$

4. The Galaxy Formation
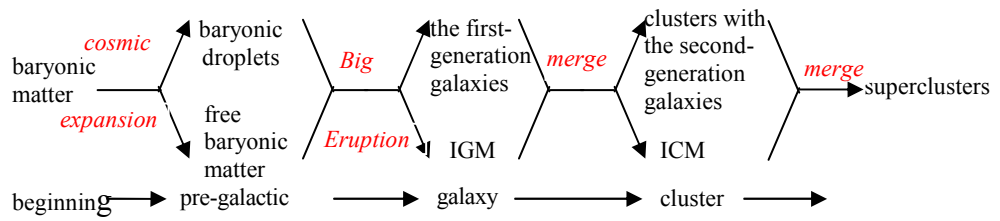
5. Extreme Force Field

$$\left(1_4\right)_m \quad + \quad \sum_{k=1}^{k} \left(\left(0_4\right)\left(1_4\right)\right)_{n,k} \qquad \xrightarrow{\text{extreme condition}}$$

particle   *gauge boson field in binary lattice space*

$$\left(1_4\right)_m \quad + \quad \sum_{k=1}^{k} \left(0_4\right)_{n,k} \left(1_4\right)_{n,k}$$

extreme particle   *extreme boson field in binary partition space*

Introduction

The unified theory of physics is the theory of everything to explain fully cosmology, dark energy, dark matter, baryonic matter, quantum mechanics, elementary particles, force fields, galaxy formation, and unusual extreme forces. The unified theory of physics is by the means of the zero-energy universe and the space-object structures.

In the zero-energy universe hypothesis, the total amount of energy in the universe is exactly zero. The conventional zero-energy universe hypothesis is based on quantum fluctuation and the exact cancellation of positive-energy matter by negative-energy gravity through pseudo-tensor [1] or the inflation [2] before the Big Bang. Quantum fluctuation provides a natural explanation for how that energy may have come out of nothing. Throughout the universe, from nothing, symmetrical particles and antiparticles spontaneously form and quickly annihilate each other without violating the law of energy conservation. Throughout the multiverse, from the zero-energy universe, symmetrical positive-energy and negative-energy universes spontaneously form and quickly annihilate each other. A negative universe becomes a negative energy gravitational field, and a positive energy universe becomes positive-energy matter as described by Stephen Hawking in A Brief History of Time [3]: "And in a sense the energy of the universe is constant; it is a constant whose value is zero. The positive energy of the matter is exactly balanced by the negative energy of the gravitational field. So the universe can start off with zero energy and still create matter."

In this paper, for our universe, the negative-energy universe is not in the form of negative-energy gravity that cancels out the positive-energy matter. The negative-energy universe is eventually in the form of dark energy that accelerates the cosmic expansion. For our universe, the zero-energy universe produced symmetrical positive-energy and negative-energy universes, which then underwent a symmetry breaking through the Higgs mechanism to generate eventually our baryonic-dark matter and dark energy, respectively. The Higgs boson can be mass-removing to convert massive particle into massless particle, or mass-giving to convert massless particle into massive particle. Before our universe, the symmetrical positive-energy and negative-energy universes coexisted. All particles were massive, the masses of all particles were equal, and our pre-universe was cold. At the beginning of our universe, the mass-removing Higgs boson converted massive particles in the positive-energy universe into massless particles, resulting in the very hot universe to initiate the Big Bang. The massive particles in the negative-energy universe remained massive. Afterward, the mass-giving Higgs boson converted some massless particles in the positive-energy universe back to massive particles. The negative-energy massive universe eventually becomes dark energy for the positive-energy universe.

Different universes in different developmental stages are the different expressions of the space-object structures. With the zero-energy universe and the space-object structures, the unified theory of physics is the unified theory of physics as the theory of everything to explain fully cosmology, dark energy, dark matter, baryonic matter, quantum mechanics, elementary particles, force fields, galaxy formation, and unusual extreme forces. The unified theory is divided into five parts: (1) the space-object structures, (2) cosmology, (3) the periodic table of elementary particles, (4) the galaxy formation, and (5) the extreme force field.

Chapter 1 deals with the space-object structures in the unified theory. The unified theory of physics is derived from the space-object structures. Different universes in different developmental stages are the different expressions of the space-object structures. Relating to rest mass, attachment space attaches to object permanently with zero speed. Relating to kinetic energy, detachment space detaches from the object at the speed of light. In our observable universe, the space structure consists of three different combinations of attachment space and detachment space, describing three different phenomena: quantum mechanics, special relativity, and the extreme force fields. The object structure consists of 11D membrane (3_{11}), 10D string (2_{10}), variable D particle ($1_{\leq 10}$), and empty object (0). The transformation among the objects is through the dimensional oscillation that involves the oscillation between high dimensional space-time with high vacuum energy and low dimensional space-time with low vacuum energy. Our observable universe with 4D space-time has zero vacuum energy.

Chapter 2 deals with cosmology. There are three stages of pre-universes in chronological order: the strong pre-universe, the gravitational pre-universe, and the charged pre-universe. The first universe from the zero-energy universe in multiverse is the strong pre-universe with the simplest expression of the space-object structures. Its object structure is 11D positive and negative membrane and its space structure is attachment space only. The only force is the pre-strong force without gravity. The transformation from 11D membrane to 10D string results in the gravitational pre-universe with both pre-strong force and pre-gravity. The repulsive pre-gravity and pre-antigravity brings about the dual 10D string universe with the bulk space. The coalescence and the separation of the dual universe result in the dual charged universe as dual 10D particle universe with the pre-strong, pre-gravity, and pre-electromagnetic force fields. The asymmetrical dimensional oscillations and the asymmetrical addition of detachment space result in the asymmetrical dual universe: the positive-energy 4D light universe with light and kinetic energy and the negative-energy oscillating 10D-4D dark universe without light and kinetic energy. The light universe is our observable universe. The dark universe is sometimes hidden, and is sometimes observable as dark energy. The dimensional oscillation for the dark universe is the slow dimensional oscillation from 10D and 4D. The dimensional oscillation for the light universe involves the immediate transformation from 10D to 4D and the introduction of detachment space, resulting in light and kinetic energy. The asymmetrical dimensional oscillation and the asymmetrical addition of detachment space are manifested as the asymmetrical weak force field. When the dark universe becomes the 4D universe, the dark universe turns into dark energy.

Chapter 3 deals with the periodic table of elementary particles. For baryonic matter, the incorporation of detachment space for baryonic matter brings about "the dimensional orbitals" as the base for the periodic table of elementary particles for all leptons, quarks, and gauge bosons. The masses of gauge bosons, leptons, quarks can be calculated using only four known constants: the number of the extra spatial dimensions in the eleven-dimensional membrane, the mass of electron, the mass of Z°, and the fine structure constant. The calculated values are in good agreement with the observed values. The differences in dimensional orbitals result in incompatible dark matter and baryonic matter. The observed new LHC Higgs Boson consists of the SM (Standard Model) Higgs boson and the hidden lepton condensate that is in the forbidden lepton family outside of the standard three-lepton families in the Standard Model. Being forbidden, a single hidden lepton cannot exist alone,

so the hidden leptons must exist in the lepton condensate as the composite of the leptons-antileptons as μ', $\bar{\mu}'$, μ'^+, and μ'^-. The decay of the hidden lepton condensate into diphoton accounts for the observed excess diphoton deviated from the Standard Model. Other decay modes of the LHC Higgs boson follow the Standard Model. The calculated masses of the hidden leptons of $\mu'^\pm$ and μ', are 120.7 GeV and 136.9 GeV, respectively, with the average as 128.8 GeV for the hidden lepton condensate in good agreements with the observed 125 or 126 GeV. The LHC Higgs boson acquires the mass of the hidden lepton condensate.

Chapter 4 deals with the formation of galaxies. The separation of dark matter without electromagnetism and baryonic matter with electromagnetism involves MOND (modified Newtonian dynamics). It is proposed that the MOND force is in the interface between the baryonic matter region and the dark matter region. In the interface, the same matter materials attract as the conventional attractive MOND force, and the different matter materials repulse as the repulsive MOND force between baryonic matter and dark matter. The source of the repulsive MOND force field is the incompatibility between baryonic matter and dark matter, like water and oil. The incompatibility does not allow the direct detection of dark matter. Typically, dark matter halo surrounds baryonic galaxy. The repulsive MOND force between baryonic matter and dark matter enhances the attractive MOND force of baryonic matter in the interface toward the center of gravity of baryonic matter. The enhancement of the low acceleration in the interface is by the acceleration constant, a_0, which defines the border of the interface and the factor of the enhancement. The enhancement of the low gravity in the interface is by the decrease of gravity with the distant rather than the square of distance as in the normal Newtonian gravity. The repulsive MOND force is the difference between the attractive MOND force and the non-existing interfacial Newtonian force. The repulsive MOND force field results in the separation and the repulsive force between baryonic matter and dark matter. The repulsive MOND force field explains the evolution of the inhomogeneous baryonic structures in the universe. Both baryonic matter and dark matter are compatible with cosmic radiation, so in the early universe, the incompatibility between baryonic matter and dark matter increases with decreasing cosmic radiation and the increasing age of the universe until reaching the maximum incompatibility. The five stages of the formation of inhomogeneous structures are free baryonic matter, baryonic droplets, the first generation galaxies by the Big Eruption, cluster, and supercluster.

Chapter 5 deals with the extreme force field. Under extreme conditions, such as the zero temperature and extremely high pressure-temperature, the extreme force fields as extreme boson force fields form. The formation of the extreme molecule (the Cooper pair) and the extreme lattice provides the mechanism for the phase transition to superconductivity, while the formation of extreme atom with electron-extreme boson provides the mechanism for the phase transition to the fractional quantum Hall effect. The formation of the stellar extreme force field in a collapsing star prevents singularity as in black hole, resulting in the formation of gravastar without singularity and with the lepton pairs-stellar extreme force field core.

1. The Space-Object Structures

The unified theory of physics unifies various phenomena in our observable universe and other universes. The unified theory of physics is derived from the space-object structures [4] [5]. All universes are governed by the space-object structures. Different universes are the different expressions of the space-object structures.

1.1. The Space Structure

The space structure [6] [7] consists of attachment space (denoted as 1) and detachment space (denoted as 0). Attachment space attaches to object permanently with zero speed. Detachment space detaches from the object at the speed of light. Attachment space relates to rest mass, while detachment space relates to kinetic energy. Different stages of our universe have different space structures.

The transformation between mass (massive particle) in attachment space and kinetic energy (massless particle) in detachment space is through the scalar Higgs boson. For example, massive particles with n units of attachment space, denoted as $(1)_n$, are converted into massless particles with n units of detachment space, denoted as $(0)_n$ through the Higgs bosons.

$$massive\ particles\ in\ (1)_n \quad \xleftrightarrow{Higgs\ Bosons} \quad massless\ particles\ in\ (0)_n \tag{1}$$

The Higgs boson can be mass-removing to convert massive particle into massless particle, or mass-giving to convert massless particle into massive particle. The Higgs boson itself is the scalar gauge boson with zero mass-energy. The virtual Higgs boson is a property of space that can turn on the transformation between the massive particle (mass-potential energy) and massless particle (kinetic energy). After the transformation, the Higgs boson remains dormant. With zero mass-energy, the Higgs boson avoids the severe problem of the huge energy (cosmological constant) from the gravity-Higgs boson interaction. The observed Higgs boson at the LHC is a remnant of the Higgs boson, not the Higgs boson itself as described later.

Our universe has both attachment space and detachment space. Before our observable universe, all particles were massive, the masses of all particles were equal, and our pre-universe was cold. At the beginning of our observable universe, the mass-removing Higgs boson converted massive particles into massless particles, resulting in the very hot universe to initiate the Big Bang. Afterward, the mass-giving Higgs boson converted some massless particles back to massive particles.

The combination of attachment space (1) and detachment space (0) brings about three different space structures: miscible space, binary partition space, and binary lattice space for four-dimensional space-time as below.

$$(1)_n\ attachment\ space\ +\ (0)_n\ \det achment\ space\ \xrightarrow{combination}$$

$$(1\,0)_n\ binary\ lattice\ space, (1+0)_n\ miscible\ space,\ or\ (1)_n(0)_n\ binary\ partition\ space \tag{2}$$

Binary lattice space, $(1\ 0)_n$, consists of repetitive units of alternative attachment space and detachment space. Thus, binary lattice space consists of multiple quantized units of attachment space separated from one another by detachment space. In miscible space, attachment space is miscible to detachment space, and there is no separation of attachment space and detachment space. Binary partition space, $(1)_n(0)_n$, consists of separated continuous phases of attachment space and detachment space.

Binary lattice space consists of multiple quantized units of attachment space separated from one another by detachment space. An object exists in multiple quantum states separated from one another by detachment space. Binary lattice space is the space for wavefunction. In wavefunction,

$$|\Psi\rangle = \sum_{i=1}^{n} c_i |\phi_i\rangle \quad , \tag{3}$$

Each individual basis element, $|\phi_i\rangle$, attaches to attachment space, and separates from the adjacent basis element by detachment space. Detachment space detaches from object. Binary lattice space with n units of four-dimensional, $(0\ \ 1)_n$, contains n units of basis elements.

Neither attachment space nor detachment space is zero in binary lattice space. The measurement in the uncertainty principle in quantum mechanics is essentially the measurement of attachment space and momentum in binary lattice space: large momentum has small non-zero attachment space, while large attachment space has low non-zero momentum. In binary lattice space, an entity is both in constant motions as wave for detachment space and in stationary state as a particle for attachment space, resulting in the wave-particle duality.

Detachment space contains no object that carries information. Without information, detachment space is outside of the realm of causality. Without causality, distance (space) and time do not matter to detachment space, resulting in non-localizable and non-countable space-time. The requirement for the system (binary lattice space) containing non-localizable and non-countable detachment space is the absence of net information by any change in the space-time of detachment space. All changes have to be coordinated to result in zero net information. This coordinated non-localized binary lattice space corresponds to nilpotent space. All changes in energy, momentum, mass, time, space have to result in zero as defined by the generalized nilpotent Dirac equation by B. M. Diaz and P. Rowlands [8].

$$(\mp \mathbf{k}\partial/\partial t \pm \mathbf{i}\nabla + \mathbf{j}m)(\pm i\mathbf{k}E \pm \mathbf{i}\mathbf{p} + \mathbf{j}m)\exp i(-Et + \mathbf{p}.\mathbf{r}) = 0 \quad , \tag{4}$$

where E, $\mathbf{p}$, m, t and $\mathbf{r}$ are respectively energy, momentum, mass, time, space and the symbols ± 1, $\pm i$, $\pm \mathbf{i}$, $\pm \mathbf{j}$, $\pm \mathbf{k}$, $\pm \mathbf{i}$, $\pm \mathbf{j}$, $\pm \mathbf{k}$, are used to represent the respective units required by the scalar, pseudoscalar, quaternion and multivariate vector groups. The changes involve the sequential iterative path from nothing (nilpotent) through conjugation, complexification, and dimensionalization. The non-local property of binary lattice space for wavefunction provides the violation of Bell inequalities [9] in quantum

mechanics in terms of faster-than-light influence and indefinite property before measurement. The non-locality in Bell inequalities does not result in net new information.

In binary lattice space, for every detachment space, there is its corresponding adjacent attachment space. Thus, no part of the object can be irreversibly separated from binary lattice space, and no part of a different object can be incorporated in binary lattice space. Binary lattice space represents coherence as wavefunction. Binary lattice space is for coherent system. Any destruction of the coherence by the addition of a different object to the object causes the collapse of binary lattice space into miscible space. The collapse is a phase transition from binary lattice space to miscible space.

$$((0)(1))_n \xrightarrow{\quad collapse \quad} (0+1)_n$$

binary lattice space   *miscible space*

(5)

Another way to convert binary lattice space into miscible space is gravity. Penrose [10] pointed out that the gravity of a small object is not strong enough to pull different states into one location. On the other hand, the gravity of large object pulls different quantum states into one location to become miscible space. Therefore, a small object without outside interference is always in binary lattice space, while a large object is never in binary lattice space.

The information in miscible space is contributed by the combination of both attachment space and detachment space, so information can no longer be non-localize. Any value in miscible space is definite. All observations in terms of measurements bring about the collapse of wavefunction, resulting in miscible space that leads to eigenvalue as definite quantized value. Such collapse corresponds to the appearance of eigenvalue, E, by a measurement operator, H, on a wavefunction, Ψ.

$$H\,\Psi \,=\, E\,\Psi \qquad , \qquad (6)$$

In miscible space, attachment space is miscible to detachment space, and there is no separation of attachment space and detachment space. In miscible space, attachment space contributes zero speed, while detachment space contributes the speed of light. A massless particle, such as photon, is on detachment space continuously, and detaches from its own space continuously. For a moving massive particle consisting of a rest massive part and a massless part, the massive part with rest mass, m_0, is in attachment space, and the massless part with kinetic energy, K, is in detachment space. The combination of the massive part in attachment space and massless part in detachment leads to the propagation speed in between zero and the speed of light.

To maintain the speed of light constant for a moving particle, the time (t) in moving particle has to be dilated, and the length (L) has to be contracted relative to the rest frame.

$$
\begin{aligned}
t &= = t_0 \Big/ \sqrt{1 - v^2/c^2} \;=\; t_0\,\gamma, \\
L &= L_0 \,/\, \gamma, \\
E &= K + m_0 c^2 = \gamma\, m_0\, c^2
\end{aligned}
$$

(7)

where $\gamma = 1/\sqrt{1-\upsilon^2/c^2}$ is the Lorentz factor for time dilation and length contraction, *E* is the total energy and *K* is the kinetic energy.

Binary partition space, $(1)_n(0)_n$, consists of separated continuous phases of attachment space and detachment space. It is for extreme force fields under extreme conditions such as near the absolute zero temperature or extremely high pressure. It will be discussed later to explain extreme phenomena such as superconductivity and black hole.

1.2. The Object Structure

The second part of the physical structures is the object structure. The object structure consists of 11D membrane (3_{11}), 10D string (2_{10}), variable D particle $(1_{4 \text{ to } 10})$, and empty object $(0_{4 \text{ to } 11})$. Different universes and different stages of a universe can have different expressions of the object structure. For an example, the four stages in the evolution of our universe are the 11D membrane universe (the strong universe), the dual 10D string universe (the gravitational pre-universe), the dual 10D particle universe (the charged pre-universe), and the dual 4D/variable D particle universe (the current universe).

The transformation among the objects is through the dimensional oscillation [5] that involves the oscillation between high dimensional space-time and low dimensional space-time. The vacuum energy of the multiverse background is about the Planck energy. Vacuum energy decreases with decreasing dimension number. The vacuum energy of 4D space-time is zero. With such vacuum energy differences, the local dimensional oscillation between high and low space-time dimensions results in local eternal expansion-contraction [11]. Eternal expansion-contraction is like harmonic oscillator, oscillating between the Planck vacuum energy and the lower vacuum energy.

For the dimensional oscillation, contraction occurs at the end of expansion. Each local region in the universe follows a particular path of the dimensional oscillation. Each path is marked by particular set of force fields. The path for our universe is marked by the strong force, gravity-antigravity, charged electromagnetism, and asymmetrical weak force, corresponding to the four stages of the cosmic evolution.

The vacuum energy differences among space-time dimensions are based on the varying speed of light. Varying speed of light has been proposed to explain the horizon problem of cosmology [12][13]. The proposal is that light traveled much faster in the distant past to allow distant regions of the expanding universe to interact since the beginning of the universe. Therefore, it was proposed as an alternative to cosmic inflation. J. D. Barrow [14] proposes that the time dependent speed of light varies as some power of the expansion scale factor *a* in such way that

$$c(t) = c_0\, a^n \tag{8}$$

where $c_0 > 0$ and *n* are constants. The increase of speed of light is continuous.

In this paper, varying dimension number (VDN) relates to quantized varying speed of light (QVSL), where the speed of light is invariant in a constant space-time

dimension number, and the speed of light varies with varying space-time dimension number from 4 to 11.

$$c_D = c / \alpha^{D-4}, \tag{9}$$

where c is the observed speed of light in the 4D space-time, c_D is the quantized varying speed of light in space-time dimension number, D, from 4 to 11, and α is the fine structure constant for electromagnetism. Each dimensional space-time has a specific speed of light. (Since from the beginning of our observable universe, the space-time dimension has always been four, there is no observable varying speed of light in our observable universe.) The speed of light increases with the increasing space-time dimension number D.

In special relativity, $E = M_0 c^2$ modified by Eq. (9) is expressed as

$$E = M_0 \cdot (c^2 / \alpha^{2(D-4)}) \tag{10a}$$

$$= (M_0 / \alpha^{2(d-4)}) \cdot c^2. \tag{10b}$$

Eq. (10a) means that a particle in the D dimensional space-time can have the superluminal speed c / α^{D-4}, which is higher than the observed speed of light c, and has the rest mass M_0. Eq. (10b) means that the same particle in the 4D space-time with the observed speed of light acquires $M_0 / \alpha^{2(d-4)}$ as the rest mass, where d = D. D in Eq. (10a) is the space-time dimension number defining the varying speed of light. In Eq. (10b), d from 4 to 11 is "mass dimension number" defining varying mass. For example, for D = 11, Eq. (10a) shows a superluminal particle in eleven-dimensional space-time, while Eq. (10b) shows that the speed of light of the same particle is the observed speed of light with the 4D space-time, and the mass dimension is eleven. In other words, 11D space-time can transform into 4D space-time with 11d mass dimension. 11D4d in Eq. (10a) becomes 4D11d in Eq. (10b) through QVSL. QVSL in terms of varying space-time dimension number, D, brings about varying mass in terms of varying mass dimension number, d.

The QVSL transformation transforms both space-time dimension number and mass dimension number. In the QVSL transformation, the decrease in the speed of light leads to the decrease in space-time dimension number and the increase of mass in terms of increasing mass dimension number from 4 to 11,

$$c_D = c_{D-n} / \alpha^{2n}, \tag{11a}$$

$$M_{0,D,d} = M_{0,D-n,\,d+n} \alpha^{2n}, \tag{11b}$$

$$D,\ d \xrightarrow{QVSL} (D \mp n),\ (d \pm n) \tag{11c}$$

where D is the space-time dimension number from 4 to 11 and d is the mass dimension number from 4 to 11. For example, in the QVSL transformation, a particle with 11D4d is transformed to a particle with 4D11d. In terms of rest mass, 11D space-time has 4d with the lowest rest mass, and 4D space-time has 11d with the highest rest mass.

Rest mass decreases with increasing space-time dimension number. The decrease in rest mass means the increase in vacuum energy, so vacuum energy increases with

12

increasing space-time dimension number. The vacuum energy of 4D particle is zero, while 11D membrane has the Planck vacuum energy.

Since the speed of light for > 4D particle is greater than the speed of light for 4D particle, the observation of > 4D particles by 4D particles violates casualty. Thus, > 4D particles are hidden particles with respect to 4D particles. Particles with different space-time dimensions are transparent and oblivious to one another, and separate from one another if possible.

1.3. Summary

The unified theory of physics is derived from the space-object structures. Different universes in different developmental stages are the different expressions of the space-object structures. Relating to rest mass, attachment space attaches to object permanently with zero speed. Relating to kinetic energy, detachment space detaches from the object at the speed of light. In our observable universe, the space structure consists of three different combinations of attachment space and detachment space, describing three different phenomena: quantum mechanics, special relativity, and the extreme force fields. The object structure consists of 11D membrane (3_{11}), 10D string (2_{10}), variable D particle ($1_{\leq 10}$), and empty object (0). The transformation among the objects is through the dimensional oscillation that involves the oscillation between high dimensional space-time with high vacuum energy and low dimensional space-time with low vacuum energy. Our observable universe with 4D space-time has zero vacuum energy.

2. Cosmology

Before the current universe, the pre-universe is in the three different stages in chronological order: the strong pre-universe, the gravitational pre-universe, and the charged pre-universe.   The strong pre-universe has only one force: the strong force.   The gravitational pre-universe has two forces: the strong and the gravitational forces.   The charged pre-universe has three forces: the strong, the gravitational, and the electromagnetic forces.   All three forces in the pre-universes are in their primitive forms unlike the finished forms in our observable universe.   The asymmetrical weak interaction comes from the formation of the current asymmetrical dual universe.   Such 4-stage cosmology for our universe explains the origin of the four force fields in our observable universe.

2.1. The Strong Pre-Universe

Dual universe	Object structure	Space structure	Force
dual	11D membrane	attachment space	pre-strong

The multiverse starts with the zero-energy universe, which produces the positive energy 11D (space-time dimensional) membrane universe and the negative energy 11D membrane universe denoted as 3_{11} 3_{-11}, as proposed by Mongan [15].   The only force among the membranes is the pre-strong force, s, as the predecessor of the strong force.   It is from the quantized vibration of the membranes to generate the reversible process of the absorption-emission of the particles among the membranes.   The pre-strong force mediates the reversible absorption-emission in the flat space.   The pre-strong force is the same for all membranes, so it is not defined by positive or negative sign.   It does not have gravity that causes instability and singularity [16], so the initial universe remains homogeneous, flat, and static.   This initial universe provides the globally stable static background state for an inhomogeneous eternal universe in which local regions undergo expansion-contraction [16].

2.2. The Gravitational Pre-Universe

Dual universe	Object structure	Space structure	Forces
dual	10D string	attachment space	pre-strong, pre-gravity

In certain regions of the 11D membrane universe, the local expansion takes place by the transformation from 11D-membrane into 10D-string.   The expansion is the result of the vacuum energy difference between 11D membrane and 10D string.   With the emergence of empty object (0_{11}), 11D membrane transforms into 10D string warped with virtue particle as pregravity.

$$3_{11}\,s \;+\; 0_{11} \quad \longleftrightarrow \quad 2_{10}\,s\,1_1 = 2_{10}\,s\,g^+ \tag{12}$$

where 3_{11} is the 11D membrane, s is the pre-strong force, 0_{11} is the 11D empty object, 2_{10} is 10D string, 1_1 is one dimensional virtue particle as g, pre-gravity.   Empty object

corresponds to the anti-De Sitter bulk space in the Randall-Sundrum model [17]. In the same way, the surrounding object can extend into empty object by the decomposition of space dimension as described by Bounias and Krasnoholovets [18], equivalent to the Randall-Sundrum model. The g is in the bulk space, which is the warped space (transverse radial space) around 2_{10}. As in the AdS/CFT duality [19] [20] [21], the pre-strong force has 10D dimension, one dimension lower than the 11D membrane, and is the conformal force defined on the conformal boundary of the bulk space. The pre-strong force mediates the reversible absorption-emission process of membrane (string) units in the flat space, while pregravity mediates the reversible condensation-decomposition process of mass-energy in the bulk space.

Through symmetry, antistrings form 10D antibranes with anti-pregravity as 2_{-10} g^-, where g^- is anti-pregravity.

$$3_{-11}\, s \; + \; 0_{-11} \; \longleftrightarrow \; 2_{-10}\, s \quad 1_{-1} = \; 2_{-10}\, s\, g^- \tag{13}$$

Pregravity can be attractive or repulsive to anti-pregravity. If it is attractive, the universe remains homogeneous. If it is repulsive, n units of $(2_{10})_n$ and n units of $(2_{-10})_n$ are separated from each other.

$$((s\,2_{10})\, g^+)_n\, (g^-\, (s\,2_{-10}))_n \tag{14}$$

The dual 10D string universe consists of two parallel universes with opposite energies: 10D strings with positive energy and 10D antistrings with negative energy. The two universes are separated by the bulk space, consisting of pregravity and anti-pregravity. There are four equal regions: positive energy string universe, pregravity bulk space, anti-pregravity bulk space, and negative energy antistring universe. Such dual universe separated by bulk space appears in the ekpyrotic universe model [22] [23].

2.3. The Charged Pre-Universe

Dual universe	Object structure	Space structure	Forces
dual	10D particle	attachment space	pre-strong, pre-gravity, pre-electromagnetic

When the local expansion stops, through the dimensional oscillation, the 10D dual universe returns to the 11D positive and negative universes, which coalesce to undergo annihilation and to return to the zero-energy universe. The 10D positive and negative universe can also coalesce to undergo annihilation and to return to the zero-energy universe. The first path of such coalescence is the annihilation, resulting in disappearance of the dual universe and the return to the zero-energy universe.

The second path allows the continuation of the dual universe in another form without the mixing of positive energy and negative energy. Such dual universe is possible by the emergence of the pre-charge force, the predecessor of electromagnetism with positive and negative charges. The mixing becomes the mixing of positive charge and negative charge instead of positive energy and negative energy, resulting in the preservation

of the dual universe with the positive energy and the negative energy. Our universe follows the second path as described below in details.

During the coalescence for the second path, the two universes coexist in the same space-time, which is predicted by the Santilli isodual theory [24]. Antiparticle for our positive energy universe is described by Santilli as follows, "this identity is at the foundation of the perception that antiparticles "appear" to exist in our space, while in reality they belong to a structurally different space coexisting within our own, thus setting the foundations of a "multidimensional universe" coexisting in the same space of our sensory perception" (Ref. [24], p. 94). Antiparticles in the positive energy universe actually come from the coexisting negative energy universe.

The mixing process follows the isodual hole theory that is the combination of the Santilli isodual theory and the Dirac hole theory. In the Dirac hole theory that is not symmetrical, the positive energy observable universe has an unobservable infinitive sea of negative energy. A hole in the unobservable infinitive sea of negative energy is the observable positive energy antiparticle.

In the dual 10D string universe, one universe has positive energy strings with pregravity, and one universe has negative energy antistrings with anti-pregravity. For the mixing of the two universes during the coalescence, a new force, the pre-charged force, emerges to provide the additional distinction between string and antistring. The pre-charged force is the predecessor of electromagnetism. Before the mixing, the positive energy string has positive pre-charge (e^+), while the negative energy antistring has negative pre-charge (e^-). During the mixing when two 10D string universes coexist, a half of positive energy strings in the positive energy universe move to the negative energy universe, and leave the Dirac holes in the positive energy universe. The negative energy antistrings that move to fill the holes become positive energy antistrings with negative pre-charge in the positive energy universe. In terms of the Dirac hole theory, the unobservable infinitive sea of negative energy is in the negative energy universe from the perspective of the positive energy universe before the mixing. The hole is due to the move of the negative energy antistring to the positive energy universe from the perspective of the positive energy universe during the mixing, resulting in the positive energy antistring with negative pre-charge in the positive energy universe.

In the same way, a half of negative energy antistrings in the negative energy universe moves to the positive energy universe, and leave the holes in the negative energy universe. The positive energy strings that move to fill the holes become negative energy strings with positive pre-charge in the negative energy universe. The result of the mixing is that both positive energy universe and the negative energy universe have strings-antistrings. The existence of the pre-charge provides the distinction between string and antistring in the string-antistring.

At that time, the space (detachment space) for radiation has not appeared in the universe, so the string-antistring annihilation does not result in radiation. The string-antistring annihilation results in the replacement of the string-antistring as the 10D string-antistring, (2_{10} 2_{-10}) by the 10D particle-antiparticle (1_{10} 1_{-10}). The 10D particles-antiparticles have the multiple dimensional Kaluza-Klein structure with variable space dimension number without the requirement for a fixed space dimension number for string-antistring. After the mixing, the dual 10D particle-antiparticle universe separated by pregravity and anti-pregravity appears as below.

$$((s\,1_{10}\ e^+\ e-\ 1_{-10}\ s)\,g^+)_n \quad (g^-(s\,1_{10}\ e^+\ e-\ 1_{-10}\ s))_n \ , \tag{15}$$

where s and e are the pre-strong force and the pre-charged force in the flat space, g is pregravity in the bulk space, and 1_{10} 1_{-10} is the particle-antiparticle.

The dual 10D particle universe consists of two parallel particle-antiparticle universes with opposite energies and the bulk space separating the two universes. There are four equal regions: the positive energy particle-antiparticle space region, the pregravity bulk space region, the negative energy particle-antiparticle space region, and the anti-pregravity bulk space region.

2.4. The Current Universe

	Object structure	Space structure	Forces
The light universe	4D particle	attachment space and detachment space	strong, gravity, electromagnetic, and weak
The dark universe	variable D between 4 and 10 particle	attachment space	pre-strong, gravity, pre-electromagnetic

The formation of our current universe follows immediately after the formation of the charged pre-universe through the asymmetrical dimensional oscillations and the asymmetrical addition of detachment space, leading to the asymmetrical dual universe. The asymmetrical dimensional oscillation involved the immediate transformation of the positive-energy universe from 10D to 4D and the slow reversible transformation of the negative-energy universe between 10D and 4D. In the asymmetrical addition of detachment space, the mass-removing Higgs boson converted massive particles in the positive-energy universe into massless particles, and the massive particles in the negative-energy universe remained massive. Afterward, the mass-giving Higgs boson converted some massless particles in the positive-energy universe back to massive particles due to mainly the CP asymmetry (particle-antiparticle asymmetry). The result was the asymmetrical dual universe consisting of the positive-energy 4D light universe with kinetic energy and light and the negative-energy oscillating 10D-4D dark universe without kinetic energy and light. The light universe contains both attachment space and detachment space.
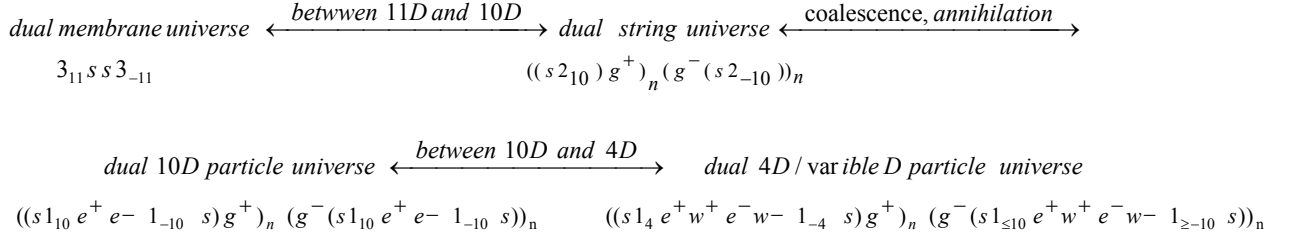
The four equal parts in the dual universe include the positive energy particle universe, the gravity bulk space, the antigravity bulk space, and the negative energy particle universe. The dark universe includes the negative energy particle universe, the antigravity bulk space, and the gravity bulk space. The light universe includes the positive energy particle universe. Therefore, the dark universe contains 75% of the total dual universe, while the light universe contains 25% of the total dual universe. The percentage (75%) of the dark universe later becomes the maximum percentage of the dark energy.

The asymmetrical dual universe is manifested as the asymmetry in the weak interaction in our observable universe as follows.

$$((s\,1_4\ e^+w^+\ e^-w-\ 1_{-4}\ s)\,g^+)_n\ (g^-\,(s\,1_{\le10}\ e^+w^+\ e^-w-\ 1_{\ge-10}\ s))_n \qquad (16)$$

where s, g, e, and w are the strong force, gravity, electromagnetism, and weak interaction, respectively for the observable universe, and where 1_41_{-4} and $1_{\le10}1_{\ge-10}$ are 4D particle-antiparticle for the light universe and variable D particle-antiparticle for the dark universe, respectively.

In summary, the whole process of the local dimensional oscillations leading to our observable universe is illustrated as follows.

dual membrane universe $\xleftarrow{\ \ betwwen\ 11D\ and\ 10D\ \ }$ *dual string universe* $\xleftarrow{\ coalescence,\ annihilation\ }$

$\qquad 3_{11}\,s\,s\,3_{-11}$ $\qquad\qquad\qquad\qquad ((s\,2_{10}\,)\,g^+)_n\,(g^-\,(s\,2_{-10}\,))_n$

dual 10D particle universe $\xleftarrow{\ \ between\ 10D\ and\ 4D\ \ }$ *dual 4D / variable D particle universe*

$((s\,1_{10}\ e^+\ e-\ 1_{-10}\ s)\,g^+)_n\ (g^-\,(s\,1_{10}\ e^+\ e-\ 1_{-10}\ s))_n$ $\qquad ((s\,1_4\ e^+w^+\ e^-w-\ 1_{-4}\ s)\,g^+)_n\ (g^-\,(s\,1_{\le10}\ e^+w^+\ e^-w-\ 1_{\ge-10}\ s))_n$

where s, e, and w are in the flat space, and g is in the bulk space. Each stage generates one force, so the four stages produce the four different forces: the strong force, gravity, electromagnetism, and the weak interaction, sequentially. Gravity appears in the first dimensional oscillation between the 11 dimensional membrane and the 10 dimensional string. The asymmetrical weak force appears in the asymmetrical second dimensional oscillation between the ten dimensional particle and the four dimensional particle. Charged electromagnetism appears as the force in the transition between the first and the second dimensional oscillations. The cosmology explains the origins of the four forces. To prevent the charged pre-universe to reverse back to the previous pre-universe, the charge pre-universe and the current universe overlap to a certain degree as shown in the overlapping between the electromagnetic interaction and the weak interaction to form the electroweak interaction.

Four-Stage Universe	Universe	Object Structure	Space Structure	Force
Strong Pre-Universe	dual	11D membrane	attachment space	pre-strong
Gravitational Pre-Universe	dual	10D string	attachment space	pre-strong, pre-gravity
Charged Pre-Universe	dual	10D particle	attachment space	pre-strong, pre-gravity, pre-electromagnetic
Current Universe	dual			
light universe		4D particle	attachment space and detachment space	strong, gravity, electromagnetic, and weak
dark universe		variable D between 4 and 10 particle	attachment space	pre-strong, gravity, pre-electromagnetic, and weak

The formation of the dark universe involves the slow dimensional oscillation between 10D and 4D. The dimensional oscillation for the formation of the dark universe involves the stepwise two-step transformation: the QVSL transformation and the varying

supersymmetry transformation. In the normal supersymmetry transformation, the repeated application of the fermion-boson transformation carries over a boson (or fermion) from one point to the same boson (or fermion) at another point at the same mass. In the "varying supersymmetry transformation", the repeated application of the fermion-boson transformation carries over a boson from one point to the boson at another point at different mass dimension number in the same space-time number. The repeated varying supersymmetry transformation carries over a boson B_d into a fermion F_d and a fermion F_d to a boson B_{d-1}, which can be expressed as follows

$$M_{d,F} = M_{d,B}\, \alpha_{d,B}, \tag{17a}$$

$$M_{d-1,B} = M_{d,F}\, \alpha_{d,F}, \tag{17b}$$

where $M_{d,B}$ and $M_{d,F}$ are the masses for a boson and a fermion, respectively, d is the mass dimension number, and $\alpha_{d,B}$ or $\alpha_{d,F}$ is the fine structure constant that is the ratio between the masses of a boson and its fermionic partner. Assuming $\alpha_{d,B}$ or $\alpha_{d,F}$, the relation between the bosons in the adjacent dimensions or n dimensions apart (assuming α's are the same) then can be expressed as

$$M_{d,B} = M_{d+1,B}\, \alpha_{d+1}^2. \tag{17c}$$

$$M_{d,B} = M_{d+n,B}\, \alpha_{d+n}^{2n}. \tag{17d}$$

$$N_{d-1} = N_d / \alpha^2. \tag{17e}$$

Eq. (18) show that it is possible to describe mass dimensions > 4 in the following way

$$F_5\, B_5\, F_6\, B_6\, F_7\, B_7\, F_8\, B_8\, F_9\, B_9\, F_{10}\, B_{10}\, F_{11}\, B_{11}, \tag{18}$$

where the energy of B_{11} is the Planck energy. Each mass dimension between 4d and 11d consists of a boson and a fermion. Eq. (19) show a stepwise transformation that converts a particle with d mass dimension to d ± 1 mass dimension.

$$D,\, d \xleftarrow{\quad stepwise \quad varying \quad supersymmetry \quad} D,\, (d \pm 1) \tag{19}$$

The transformation from a higher mass dimensional particle to the adjacent lower mass dimensional particle is the fractionalization of the higher dimensional particle to the many lower dimensional particles in such way that the number of lower dimensional particles becomes $N_{d-1} = N_d / \alpha^2$. The transformation from lower dimensional particles to higher dimensional particle is a condensation. Both the fractionalization and the condensation are stepwise. For example, a particle with 4D (space-time) 10d (mass dimension) can transform stepwise into 4D9d particles. Since the supersymmetry transformation involves translation, this stepwise varying supersymmetry transformation leads to a translational fractionalization and translational condensation, resulting in expansion and contraction.

For the formation of the dark universe from the charged pre-universe, the negative energy universe has the 10D4d particles, which is converted eventually into 4D4d stepwise and slowly. It involves the stepwise two-step varying transformation: first the QVSL transformation, and then, the varying supersymmetry transformation as follows.

$$\text{stepwise two-step varying transformation}$$

$$(1)\quad D, d \xleftrightarrow{\quad QVSL \quad} (D \mp 1), \ (d \pm 1) \tag{20}$$

$$(2)\quad D, d \xleftrightarrow{\quad \text{varying supersymmetry} \quad} D, (d \pm 1)$$

The repetitive stepwise two-step transformations from 10D4d to 4D4d are as follows.

The Hidden Dark Universe and the Observable Dark Universe with Dark Energy

$$10D4d \rightarrow 9D5d \rightarrow 9D4d \rightarrow 8D5d \rightarrow 8D4d \rightarrow 7D5d \rightarrow \bullet \bullet \bullet \bullet \rightarrow 5D4d \rightarrow 4D5d \rightarrow 4D4d$$
$$\mapsto \quad the \qquad hidden \qquad\quad dark \qquad\qquad universe \leftarrow\mapsto dark\ energy \leftarrow$$

The dark universe consists of two periods: the hidden dark universe and the dark energy universe. The hidden dark universe composes of the $> 4D$ particles. As mentioned before, particles with different space-time dimensions are transparent and oblivious to one another, and separate from one another if possible. Thus, $> 4D$ particles are hidden and separated particles with respect to 4D particles in the light universe (our observable universe). The universe with $> 4D$ particles is the hidden dark universe. The 4D particles transformed from hidden $> 4D$ particles in the dark universe are observable dark energy for the light universe, resulting in the accelerated expanding universe. The accelerated expanding universe consists of the positive energy 4D particles-antiparticles and dark energy that includes the negative energy 4D particles-antiparticles and the antigravity. Since the dark universe does not have detachment space, the presence of dark energy is not different from the presence of the non-zero vacuum energy. In terms of quintessence, such dark energy can be considered the tracking quintessence [25] from the dark universe with the space-time dimension as the tracker. The tracking quintessence consists of the hidden quintessence and the observable quintessence. The hidden quintessence is from the hidden $> 4D$ dark universe. The observable quintessence is from the observable 4D dark universe with 4D space-time.

For the formation of the light universe, the dimensional oscillation for the positive energy universe transforms 10D to 4D immediately. It involves the leaping two-step varying transformation, resulting in the light universe with kinetic energy. The first step is the space-time dimensional oscillation through QVSL. The second step is the mass dimensional oscillation through slicing-fusion.

$$\textit{leaping two-step varying transformation}$$

$$(1)\quad D, d \xleftrightarrow{\quad QVSL \quad} (D \mp n), \ (d \pm n) \tag{21}$$

$$(2)\quad D, d \xleftrightarrow{\quad \text{slicing-fusion} \quad} D, (d \pm n) + (11 - d + n)\,DO's$$

The Light Universe

$$10D4d \xrightarrow{\quad quick \ QVSL \ transforma\,tion \quad} 4D10d \xrightarrow{\quad slicing \ with \ \det achment \ space\,, \inf lation \quad}$$

$$dark \ matter \ (4D9d + 4D8d + 4D7d + 4D6d + 4D5d) \ + baryonic \ matter \ (4D4d) + cosmic \ radiation$$

$$\rightarrow thermal \ cos mic \ exp ansion \ (the \ Big \ Bang\,)$$

In the charged pre-universe, the positive energy universe has 10D4d, which is transformed into 4D10d in the first step through the QVSL transformation. The second step of the leaping varying transformation involves the slicing-fusion of particle. Bounias and Krasnoholovets [26] propose another explanation of the reduction of > 4 D space-time into 4D space-time by slicing > 4D space-time into infinitely many 4D quantized units surrounding the 4D core particle. Such slicing of > 4D space-time is like slicing 3-space D object into 2-space D object in the way stated by Michel Bounias as follows: "You cannot put a pot into a sheet without changing the shape of the 2-D sheet into a 3-D dimensional packet. Only a 2-D slice of the pot could be a part of sheet".

The slicing is by detachment space, as a part of the space structure, which consists of attachment space (denoted as 1) and detachment space (denoted as 0) as described earlier. Attachment space attaches to object permanently with zero speed. Detachment space detaches from the object at the speed of light. Attachment space relates to rest mass, while detachment space relates to kinetic energy.   The cosmic origin of detachment space is the cosmic radiation from the particle-antiparticle annihilation that initiates the transformation. The cosmic radiation cannot permanently attach to a space.

The slicing of dimensions is the slicing of mass dimensions. 4D10d particle is sliced into six particles: 4D9d, 4D8d, 4D7d, 4D6d, 4D5d, and 4D4d equally by mass. Baryonic matter is 4D4d, while dark matter consists of the other five types of particles (4D9d, 4D8d, 4D7d, 4D6d, and 4D5d) as described later. The mass ratio of dark matter to baryonic matter is 5 to 1 in agreement with the observation [27] showing the universe consists of 22.7% dark matter, 4.56% baryonic matter, and 72.8% dark energy.

Detachment space (0) involves in the slicing of mass dimensions. Attachment space is denoted as 1. For example, the slicing of 4D10d particles into 4D4d particles is as follows.

$$\left(1_{4+6}\right)_i \xrightarrow{\quad slicing \quad} \left(1_4\right)_i \quad + \quad \sum_1^6 \left(\left(0_4\right)\left(1_4\right)\right)_{j,6}$$

$$> 4d \ attachment \ space \qquad 4d \ core \ attachment \ space \qquad 6 \ types \ of \ 4d \ units \qquad (22)$$

The two products of the slicing are the 4d-core attachment space and 6 types of 4d quantized units. The 4d core attachment space surrounded by 6 types of many (j) 4D4d quantized units corresponds to the core particle surrounded by 6 types of many small 4d particles.

Therefore, the transformation from d to d − n involves the slicing of a particle with d mass dimension into two parts: the core particle with d − n dimension and the n dimensions that are separable from the core particle. Such n dimensions are denoted as n "dimensional orbitals", which become gauge force fields as described later. The sum of the number of mass dimensions for a particle and the number of dimensional orbitals (DO's) is equal to 11 (including gravity) for all particles with mass dimensions. Therefore,

$$F_d = F_{d-n} + (11 - d + n)\,DO's \tag{23}$$

where $11 - d + n$ is the number of dimensional orbitals (DO's) for F_{d-n}. Thus, 4D10d particles can transformed into 4D9d, 4D8d, 4D7d, 4D6d, 4D5d, and 4D4d core particles, which have 2, 3, 4, 5, 6, and 7 separable dimensional orbitals, respectively. 4D4d has gravity and six other dimensional orbitals as gauge force fields as below.

The six > 4d mass dimensions (dimensional orbitals) for the gauge force fields and the one mass dimension for gravity are as in Figure 1.

Figure 1. The seven force fields as > 4d mass dimensions (dimensional orbitals).

The dimensional orbitals of baryonic matter provide the base for the periodic table of elementary particles to calculate accurately the masses of all 4D elementary particles, including quarks, leptons, and gauge bosons as described later.

The lowest dimensional orbital is for electromagnetism. Baryonic matter is the only one with the lowest dimensional orbital for electromagnetism. With higher dimensional orbitals, dark matter does not have this lowest dimensional orbital. Without electromagnetism, dark matter cannot emit light, and is incompatible to baryonic matter, like the incompatibility between oil and water. The incompatibility between dark matter and baryonic matter leads to the inhomogeneity (like emulsion), resulting in the formation of galaxies, clusters, and superclusters as described later. Dark matter has not been found by direct detection because of the incompatibility.

In the light universe, the inflation is the leaping varying transformation that is the two-step inflation. The first step is to increase the rest mass as potential from higher space-time dimension to lower space-time dimension as expressed by Eq. (24a) from Eq. (11b).

$$D,\,d \xrightarrow{\ QVSL\ } (D \mp n),\ (d \pm n)$$
$$V_{D,d} = V_{D-n,\,d+n}\,\alpha^{2n}$$
$$\varphi = collective\ n's$$
$$V(\varphi) = V_{4D10d}\,\alpha^{-2\varphi},\ where\ \varphi \le 0\ from -6\ to\ 0$$

$$\tag{24a}$$

where α is the fine structure constant for electromagnetism. The ratio of the potential energies of 4D10d to that of 10D4d is $1/\alpha^{12}$. φ is the scalar field for QVSL, and is equal to collective n's as the changes in space-time dimension number for many particles. The increase in the change of space-time dimensions from 4D decreases the potential as the rest mass. The region for QVSL is $\varphi \le 0$ from -6 to 0. The QVSL region is for the conversion of the vacuum energy into the rest mass as the potential.

The second step is the slicing that occurs simultaneously with the appearance of detachment space that is the space for cosmic radiation (photon). Potential energy as

massive 4D10d particles is converted into kinetic energy as cosmic radiation and massive matter particles (from 10d to 4d). It relates to the ratio between photon and matter in terms of the CP asymmetry between particle and antiparticle. The slight excess particle over antiparticle results in matter particle. The equation for the potential (V) and the scalar field (ϕ) is as Eq. (24b) from Eq. (35) that expresses the ratio between photon and matter.

$$D, d \xrightarrow{\text{slicing}} D, (d-n)$$

$$V(\phi) = V_{4D10d}\,\alpha^{2\phi}\,, where\ \phi \geq 0\ from\ 0\ to\ 2 \tag{24b}$$

The ratio is α^4, according to Eq. (35). The region for the slicing is $\phi \geq 0$ from 0 to 2. The slicing region is for the conversion of the potential energy into the kinetic energy.

The combination of Eq. (24a) and Eq. (24b) is as Eq. (24c).

$$V(\varphi,\phi) = V_{4D10d}\,(\alpha^{-2\varphi} + \alpha^{2\phi}),$$
$$where\ \varphi \leq 0\ and\ \phi \geq 0 \tag{24c}$$

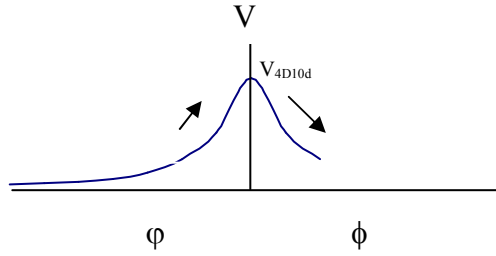The graph for the two-step inflation is as Figure 2.

Figure 2. the two-step inflation

At the transition (V_{4D10d}) between the first step (QVSL) and the second step (slicing), the scalar field reverses its sign and direction. In the first step, the universe inflates by the decrease in vacuum energy. In the second step, the potential energy is converted into kinetic energy as cosmic radiation. The resulting kinetic energy starts the Big Bang, resulting in the expanding universe.

Toward the end of the cosmic contraction after the big crunch, the deflation occurs as the opposite of the inflation. The kinetic energy from cosmic radiation decreases, as the fusion occurs to eliminate detachment space, resulting in the increase of potential energy. At the end of the fusion, the force fields except gravity disappear, 4D10d particles appear, and then the scalar field reverses its sign and direction. The vacuum energy increases as the potential as the rest mass decreases for the appearance of 10D4d particles, resulting in the end of a dimensional oscillation as Figure 3 for the two-step deflation.
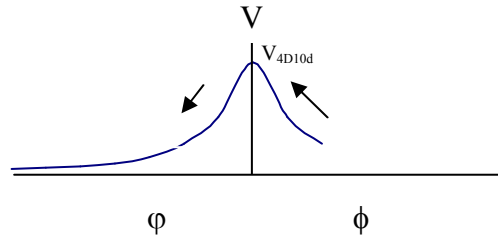

Figure 3. the two-step deflation

The end of the two-step deflation is 10D4d, which is followed immediately by the dimensional oscillation to return to 4D10d as the "dimensional bounce" as shown in Figure 4, which describes the dimensional oscillation from the left to the right: the beginning (inflation as 10D4d through 4D10d to 4D4d), the cosmic expansion-contraction, the end (deflation as 4D4d through 4D10d to 10D4d), the beginning (inflation), the cosmic expansion-contraction, and the end (deflation).
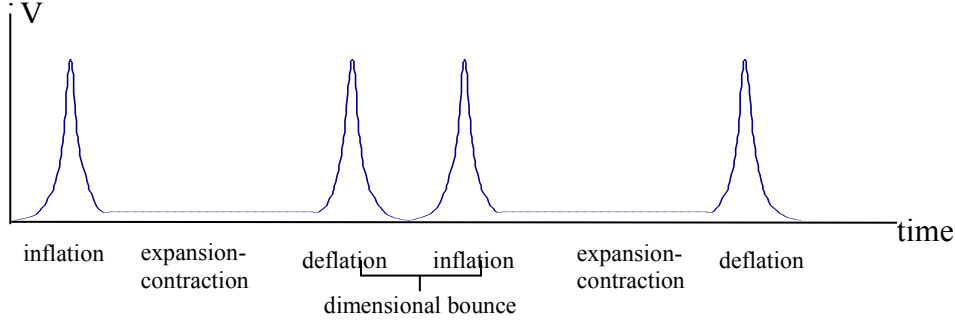

Figure 4. the cyclic observable universe by the dimensional oscillation

The two-step inflation corresponds to the quintom inflation. The symmetry breaking for the light universe can be described by quintom. Quintom [28] [29] [30] is the combination of quintessence and phantom. Quintessence describes a time-varying equation of state parameter, w, the ratio of its pressure to energy density and $w > -1$.

$$L_{quint\,essnec} = \frac{1}{2}(\partial_{\mu}\phi)^2 - V(\phi) \tag{25}$$

$$w = \frac{\dot{\phi}^2 - 2V(\phi)}{\dot{\phi}^2 + 2V(\phi)} \tag{26}$$

$$-1 \le w \le +1$$

Quintom includes phantom with $w < -1$. It has opposite sign of kinetic energy.

$$L_{phantom} = \frac{-1}{2}(\partial_{\mu}\varphi)^2 - V(\varphi) \tag{27}$$

$$w = \frac{-\dot{\varphi}^2 - 2V(\varphi)}{-\dot{\varphi}^2 + 2V(\varphi)} \tag{28}$$

$$-1 \ge w$$

As the combination of quintessence and phantom from Eqs. (24), (25), (26), and (27), quintom is as follows.

$$L_{quint\,essnec} = \frac{1}{2}(\partial_{\mu}\phi)^2 - \frac{1}{2}(\partial_{\mu}\varphi)^2 - V(\phi) - V(\varphi) \tag{29}$$

24

$$w = \frac{\dot{\phi}^2 - \dot{\varphi}^2 - 2V(\phi) - 2V(\varphi)}{\dot{\phi}^2 - \dot{\varphi}^2 + 2V(\phi) + 2V(\varphi)} \tag{30}$$

Phantom represents the scalar field φ in the space-time dimensional oscillation in QVSL, while quintessence represents the scalar field ϕ in the mass dimensional oscillation in the slicing-fusion. Since QVSL does not involve kinetic energy, the physical source of the negative kinetic energy for phantom is the increase in vacuum energy, resulting in the decrease in energy density and pressure with respect to the observable potential, $V(\varphi)$. Combining Eqs. (24c) and (30), quintom is as follows.

$$w = \frac{\dot{\phi}^2 - \dot{\varphi}^2 - 2V(\phi) - 2V(\varphi)}{\dot{\phi}^2 - \dot{\varphi}^2 + 2V(\phi) + 2V(\varphi)}$$

$$= \frac{\dot{\phi}^2 - \dot{\varphi}^2 - 2V_{4D10d}(\alpha^{-2\varphi} + \alpha^{2\phi})}{\dot{\phi}^2 - \dot{\varphi}^2 + 2V_{4D10d}(\alpha^{-2\varphi} + \alpha^{2\phi})} \tag{31}$$

where $\varphi \leq 0$ and $\phi \geq 0$

Figure 5 shows the plot of the evolution of the equation of state w for the quintom inflation.
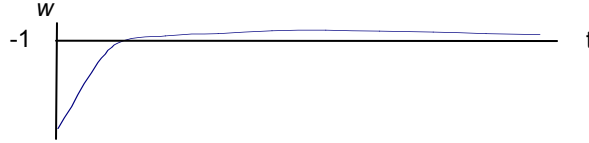

Figure 5. the w of quintom for the quintom inflation

Figure 6 shows the plot of the evolution of the equation of state w for the cyclic universe as Figure 4.
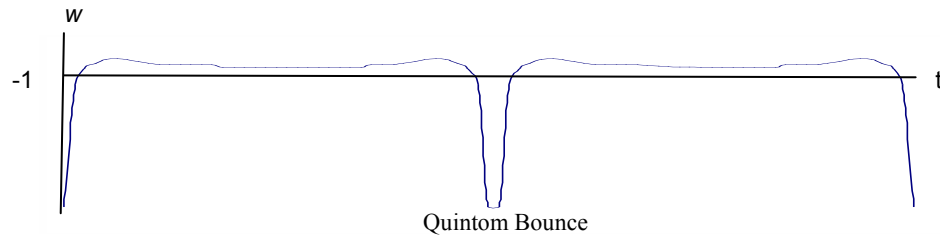

Figure 6. the cyclic universe by the dimensional oscillation as Figure 4

In the dimensional bounce in the middle of Figure 6, the equation of state crosses $w = -1$ twice as also shown in the recent development of the quintom model [31] [32] in which, for the Quintom Bounce, the equation of state crosses the cosmological constant boundary twice around the bounce point to start another cycle of the dual universe.

The hidden dark universe with D > 4 and the observable universe with D = 4 are the "parallel universes" separated from each other by the bulk space. When the slow QVSL transformation transforms gradually 5D hidden particles in the hidden universe into observable 4D particles, and the observable 4 D particles become the dark energy for

the observable universe starting from about 5 billion years ago (more precisely 4.71 ± 0.98 billion years ago at z = 0.46 ± 0.13) [33]. At a certain time, the hidden universe disappears, and becomes completely observable as dark energy. The maximum connection of the two universes includes the positive energy particle-antiparticle space region, the gravity bulk space region, the negative energy particle-antiparticle space region, and the anti-gravity bulk space region. Through the symmetry among the space regions, all regions expand synchronically and equally. (The symmetry is necessary for the ultimate reversibility of all cosmic processes.)

The light universe includes the positive-energy particle-antiparticle universe, and the dark universe includes the negative-energy particle-antiparticle universe, the anti-gravity bulk space, and the gravity bulk space. The light universe occupies 25% of the total universe, while the dark universe occupies 75% of the total universe, so the maximum dark energy from the dark universe is 75%. The present observable universe about reaches the maximum (75%) at the observed 72.8% dark energy [27]. At 72.8% dark energy, the calculated values for baryonic matter and dark matter (with the 1:5 ratio) are 4.53% (= (100 – 72.8)/6) and 22.7% (= 4.53 x 5), respectively, in excellent agreement with observed 4.56% and 22.7%, respectively [27]. Our universe is 13.7 billion-year old. Dark energy as the transformation from 5D to 4D started in about 4.71 ± 0.98 billion years ago [33]. The ratio of the time periods for the transformations from D → D - 1 is proportional to ln of the total number of particles (Eqs. (11b) and (17e)) to be transformed from D → D − 1 for the exponential growth with time.

The Percentages of the Periods in the Dark Universe

	10D $\rightarrow$ 9D	9D $\rightarrow$ 8D	8D $\rightarrow$ 7D	7D $\rightarrow$ 6D	6D $\rightarrow$ 5D	5D $\rightarrow$ 4D
ratio of total numbers of particles	1	α^{-2}	α^{-4}	α^{-6}	α^{-8}	α^{-10}
ratio of ln (total number of particles)	0	-2α	-4α	-6α	-8α	-10α
ratio of periods	~0	1	2	3	4	5
percentages of periods	~0	6.7	13.3	20	26.7	33.3

α is the fine structure constant for electromagnetism from Eq. (11b)

The period of the 5D → 4D is (0.333) (13.7)/ ((0.333) (72.8/75) + 0.667) = 4.61 billion years, and dark energy as the 5D → 4D started in (4.61) (72.8/75) = 4.47 billon years ago that is in agreement with the observed value of 4.71 ± 0.98 billion years ago [33].

After the maximally connected universe, 4D dark energy transforms back to > 4D particles that are not observable. The removal of dark energy in the observable universe results in the stop of accelerated expansion and the start of contraction of the observable universe.

The end of dark energy starts another "parallel universe period". Both hidden universe and observable universe contract synchronically and equally. Eventually, gravity causes the observable universe to crush to lose all cosmic radiation, resulting in the return to 4D10d particles under the deflation. The increase in vacuum energy allows 4D10d particles to become positive energy 10D4d particles-antiparticle. Meanwhile, hidden > 4D particles-antiparticles in the hidden universe transform into negative energy 10D4d particles-antiparticles. The dual universe can undergo another cycle of the dual universe with the dark and light universes. On the other hand, both universes can

undergo transformation by the reverse isodual hole theory to become dual 10D string universe, which in turn can return to the 11D membrane universe that in turn can return to the zero-energy universe as follows.
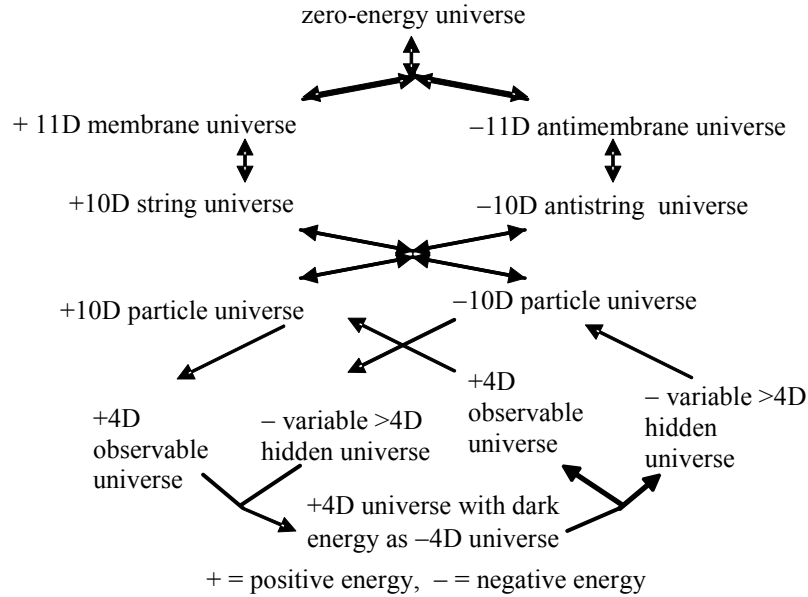
zero-energy universe

+ 11D membrane universe   −11D antimembrane universe

+10D string universe   −10D antistring universe

+10D particle universe   −10D particle universe

+4D observable universe

− variable >4D hidden universe

+4D observable universe

− variable >4D hidden universe

+4D universe with dark energy as −4D universe

+ = positive energy, − = negative energy

Figure 7. Cosmology

2.5. Summary

There are three stages of pre-universes in chronological order: the strong pre-universe, the gravitational pre-universe, and the charged pre-universe. The first universe from the zero-energy universe in multiverse is the strong pre-universe with the simplest expression of the space-object structures.   Its object structure is 11D positive and negative membrane and its space structure is attachment space only. The only force is the pre-strong force without gravity. The transformation from 11D membrane to 10D string results in the gravitational pre-universe with both pre-strong force and pre-gravity. The repulsive pre-gravity and pre-antigravity brings about the dual 10D string universe with the bulk space. The coalescence and the separation of the dual universe result in the dual charged universe as dual 10D particle universe with the pre-strong, pre-gravity, and pre-electromagnetic force fields.

The asymmetrical dimensional oscillations and the asymmetrical addition of detachment space result in the asymmetrical dual universe: the positive-energy 4D light universe with light and kinetic energy and the negative-energy oscillating 10D-4D dark universe without light and kinetic energy. The light universe is our observable universe. The dark universe is sometimes hidden, and is sometimes observable as dark energy. The dimensional oscillation for the dark universe is the slow dimensional oscillation from 10D and 4D. The dimensional oscillation for the light universe involves the immediate transformation from 10D to 4D and the introduction of detachment space, resulting in light and kinetic energy. The asymmetrical dimensional oscillation and the asymmetrical

27

addition of detachment space are manifested as the asymmetrical weak force field. When the dark universe becomes the 4D universe, the dark universe turns into dark energy. The calculated percentages of dark energy, dark matter, and baryonic matter 72.8, 22.7, and 4.53, respectively, in nearly complete agreement with observed 72.8, 22.7, and 4.56, respectively. According to the calculation, dark energy started in 4.47 billion years ago in agreement with the observed 4.71 ± 0.98 billion years ago.

3. The Periodic Table of Elementary Particles

3.1. The CP Asymmetry

In the light universe, cosmic radiation is the result of the annihilation of the CP symmetrical particle-antiparticle. However, there is the CP asymmetry, resulting in excess of matter. Matter results from the combination of the CP asymmetrical particle-antiparticle. A baryonic matter particle (4d) has seven dimensional orbitals. The CP asymmetrical particle-antiparticle particle means the combination of two asymmetrical sets of seven from particle and antiparticle, resulting in the combination of the seven "principal dimensional orbitals" and the seven "auxiliary dimensional orbitals". The auxiliary orbitals are dependent on the principal orbitals, so a baryonic matter particle appears to have only one set of dimensional orbitals. For baryonic matter, the principal dimensional orbitals are for leptons and gauge bosons, and the auxiliary dimensional orbitals are mainly for individual quarks. Because of the dependence of the auxiliary dimensional orbitals, individual quarks are hidden. In other words, there is asymmetry between lepton and quark, resulting in the survival of matter without annihilation. The configuration of dimensional orbitals and the periodical table of elementary particles [34] are shown in Fig. 8 and Table 1.
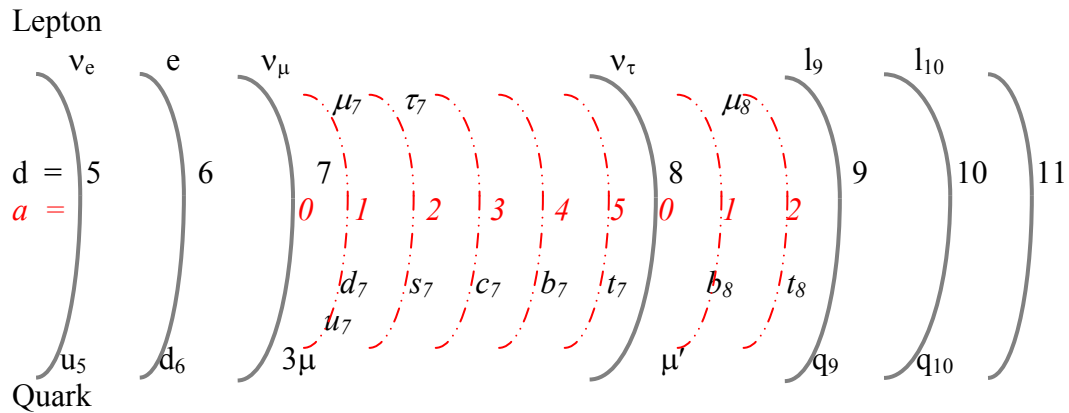

Fig. 8: leptons and quarks in the principal and auxiliary dimensional orbitals   d = principal dimensional orbital (solid line) number, a = auxiliary dimensional orbital (dot line) number

Table 1. The Periodic Table of Elementary Particles
d = principal dimensional orbital number, a = auxiliary dimensional orbital number

D	a = 0	1	2	a = 0	1	2	3	4	5	
	Lepton			Quark						Boson
5	$L_5 = \nu_e$			$q_5 = u = 3\nu_e$						$B_5 = A$
6	$L_6 = e$			$q_6 = d = 3e$						$B_6 = \pi_{1/2}$
7	$L_7 = \nu_\mu$	μ_7	τ_7	$q_7 = 3\mu$	u_7/d_7	s_7	c_7	b_7	t_7	$B_7 = Z_L^{\,0}$
8	$L_8 = \nu_\tau$	μ_8		$q_8 = \mu'$	b_8	t_8				$B_8 = X_R$
		(empty)			(empty)					
9	L_9			q_9						$B_9 = X_L$
10										$B_{10} = Z_R^{\,0}$
11										B_{11}

In Fig. 8 and Table 1, d is the principal dimensional orbital number, and a is the auxiliary dimensional orbital number. (Note that F_d has lower energy than B_d.)

3.2. The Boson Mass Formula

The principal dimensional orbitals are for gauge bosons of the force fields. For the gauge bosons, the seven orbitals of principal dimensional orbital are arranged as F_5 B_5 F_6 B_6 F_7 B_7 F_8 B_8 F_9 B_9 F_{10} B_{10} F_{11} B_{11}, where B and F are boson and fermion in each orbital. The mass dimension in Eq. (17) becomes the orbitals in dimensional orbital with the same equations.

$$M_{d,F} = M_{d,B}\, \alpha_{d,B}, \tag{32a}$$

$$M_{d-1,B} = M_{d,F}\, \alpha_{d,F}, \tag{32b}$$

$$M_{d-1,B} = M_{d,B}\, \alpha_d^2. \tag{32c}$$

where D is the dimensional orbital number from 6 to 11. $E_{5,B}$ and $E_{11,B}$ are the energies for the 5d dimensional orbital and the 11d dimensional orbital, respectively. The lowest energy is the Coulombic field,

$$E_{5,B} = \alpha\, E_{6,F} = \alpha\, M_e. \tag{33}$$

The bosons generated are the dimensional orbital bosons or B_D. Using only α_e, the mass of electron (M_e), the mass of Z^0, and the number (seven) of dimensional orbitals, the masses of B_D as the gauge boson can be calculated as shown in Table 2.

Table 2. The Masses of the dimensional orbital bosons:
$\alpha = \alpha_e$, d = dimensional orbital number

B_d	M_d	GeV (calculated)	Gauge boson	Interaction, symmetry	Predecessor
B_5	$M_e\,\alpha$	3.7×10^{-6}	A	Electromagnetic, U(1)	Pre-charged
B_6	M_e/α	7×10^{-2}	$\pi_{1/2}$	Strong, SU(3)	Pre-strong
B_7	$M_6/\alpha_w^2 \cos\theta_w$	91.177 (given)	Z_L^0	weak (left), SU(2)$_L$	Fractionalization (slicing)
B_8	M_7/α^2	1.7×10^6	X_R	CP (right) nonconservation	CP asymmetry
B_9	M_8/α^2	3.2×10^{10}	X_L	CP (left) nonconservation	CP asymmetry
B_{10}	M_9/α^2	6.0×10^{14}	Z_R^0	weak (right)	Fractionalization (slicing)
B_{11}	M_{10}/α^2	1.1×10^{19}	G	Gravity	Pregravity

In Table 2, $\alpha = \alpha_e$ (the fine structure constant for electromagnetic field), and $\alpha_w = \alpha/\sin^2\theta_w$. α_w is not same as α of the rest, because as shown later, there is a mixing between B_5 and B_7 as the symmetry mixing between U(1) and SU(2) in the standard theory of the electroweak interaction, and $\sin\theta_w$ is not equal to 1. (The symmetrical charged dual pre-universe overlaps with the current asymmetrical universe for the weak interaction as shown earlier.) As shown later, B_5, B_6, B_7, B_8, B_9, and B_{10} are A (massless photon), $\pi_{1/2}$ (half of pion), Z_L^0, X_R, X_L, and Z_R^0, respectively, responsible for the electromagnetic field, the strong interaction, the weak (left handed) interaction, the CP (right handed) nonconservation, the CP (left handed) nonconservation, and the P (right handed) nonconservation, respectively. The calculated value for α_w is 0.2973, and θ_w is 29.69^0 in good agreement with 29.31^0 for the observed value of θ_w [35]. The calculated energy for B_{11} is 1.1×10^{19} GeV in good agreement with the Planck mass, 1.2×10^{19} GeV. The strong interaction, representing by $\pi_{1/2}$ (half of pion), is for the interactions among quarks, and for the hiding of individual quarks in the auxiliary orbital. The weak interaction, representing by Z_L^0, is for the interaction involving changing flavors (decomposition and condensation) among quarks and leptons.

There are dualities between dimensional orbitals and the cosmic evolution process. The pre-charged force, the pre-strong force, the fractionalization, the CP asymmetry, and the pregravity are the predecessors of electromagnetic force, the strong force, the weak interaction, the CP nonconservation, and gravity, respectively. These forces are manifested in the dimensional orbitals with various space-time symmetries and gauge symmetries. The strengths of these forces are different than their predecessors, and are arranged according to the dimensional orbitals. Only the 4d particle (baryonic matter) has the B_5, so without B_5, dark matter consists of permanently neutral higher dimensional particles. It cannot emit light, cannot form atoms, and exists as neutral gas.

The principal dimensional boson, B_8, is a CP violating boson, because B_8 is assumed to have the CP-violating U(1)$_R$ symmetry. The ratio of the force constants between the CP-invariant W_L in B_8 and the CP-violating X_R in B_8 is

$$\frac{G_8}{G_7} = \frac{\alpha \ E_7^2 \ \cos^2 \Theta_W}{\alpha_W \ E_8^2}$$

$$= 5.3 \ X \ 10^{-10} \quad , \tag{34}$$

which is in the same order as the ratio of the force constants between the CP-invariant weak interaction and the CP-violating interaction with $|\Delta S| = 2$.

The principal dimensional boson, B_9 (X_L), has the CP-violating U(1)$_L$ symmetry. B_9 generates matter. The ratio of force constants between X_R with CP conservation and X_L with CP-nonconservation is

$$\frac{G_9}{G_8} = \frac{\alpha E_8^2}{\alpha E_9^2}$$

$$= \alpha^4 \tag{35}$$

$$= 2.8 \ X \ 10^{-9} \quad ,$$

which is the ratio of the numbers between matter (dark and baryonic) and photons in the universe. It is close to the ratio of the numbers between baryonic matter and photons about 5×10^{-10} obtained by the Big Bang nucleosynthesis.

Auxiliary dimensional orbital is derived from principal dimensional orbital. It is for high-mass leptons and individual quarks. The combination of dimensional auxiliary dimensional orbitals constitutes the periodic table for elementary particles as shown in Fig. 8 and Table 1.

There are two types of fermions in the periodic table of elementary particles: low-mass leptons and high-mass leptons and quarks. Low-mass leptons include ν_e, e, ν_μ, and ν_τ, which are in principal dimensional orbital, not in auxiliary dimensional orbital. l_d is denoted as lepton with principal dimension number, d. l_5, l_6, l_7, and l_8 are ν_e, e, ν_μ, and ν_τ, respectively. All neutrinos have zero mass because of chiral symmetry (permanent chiral symmetry).

3.3. The Mass Composites of Leptons and Quarks

High-mass leptons and quarks include μ, τ, u, d, s, c, b, and t, which are the combinations of both principal dimensional fermions and auxiliary dimensional fermions. Each fermion can be defined by principal dimensional orbital numbers (d's) and auxiliary dimensional orbital numbers (a's) as d_a in Table 3. For examples, e is 6_0 that means it has d (principal dimensional orbital number) = 6 and a (auxiliary dimensional orbital number) = 0, so e is a principal dimensional fermion.

High-mass leptons, μ and τ, are the combinations of principal dimensional fermions, e and ν_μ, and auxiliary dimensional fermions. For example, μ is the combination of e, ν_μ, and μ_7, which is 7_1 that has d = 7 and a = 1 .

Quarks are the combination of principal dimensional quarks (q_d) and auxiliary dimensional quarks. The principal dimensional fermion for quark is derived from principal dimensional lepton. To generate a principal dimensional quark in principal dimensional orbital from a lepton in the same principal dimensional orbital is to add the lepton to the boson from the combined lepton-antilepton. Thus, the mass of the quark is three times of

the mass of the corresponding lepton in the same dimension. The equation for the mass of principal dimensional fermion for quark is

$$M_{q_d} = 3M_{l_d} \tag{36}$$

For principal dimensional quarks, q_5 (5_0) and q_6 (6_0) are $3\nu_e$ and $3e$, respectively. Since l_7 is massless ν_μ, ν_μ is replaced by μ, and q_7 is 3μ. Quarks are the combinations of principal dimensional quarks, q_d, and auxiliary dimensional quarks. For example, s quark is the combination of q_6 (3e), q_7 (3μ) and s_7 (auxiliary dimensional quark = 7_2).

Each fermion can be defined by principal dimensional orbital numbers (d's) and auxiliary dimensional orbital numbers (a's). All leptons and quarks with d's, a's and the calculated masses are listed in Table 3.

Table 3. The Compositions and the Constituent Masses of Leptons and Quarks
d = principal dimensional orbital number and a = auxiliary dimensional orbital number

	d_a	Composition	Calculated Mass
Leptons	d_a for leptons		
ν_e	5_0	ν_e	0
e	6_0	e	0.51 MeV (given)
ν_μ	7_0	ν_μ	0
ν_τ	8_0	ν_τ	0
μ	$6_0 + 7_0 + 7_1$	$e + \nu_\mu + \mu_7$	105.6 MeV
τ	$6_0 + 7_0 + 7_2$	$e + \nu_\mu + \tau_7$	1786 MeV
μ'	$6_0 + 7_0 + 7_2 + 8_0 + 8_1$	$e + \nu_\mu + \mu_7 + \nu_\tau + \mu_{8\ (3/2\ Z°)}$	136.9 GeV
$\mu'^\pm$	$6_0 + 7_0 + 7_2 + 8_0 + 8_1{}^\pm$	$e + \nu_\mu + \mu_7 + \nu_\tau + \mu_8{}^\pm{}_{(3/2\ W^\pm)}$	120.7 GeV
Quarks	d_a for quarks		
u	$5_0 + 7_0 + 7_1$	$q_5 + q_7 + u_7$	330.8 MeV
d	$6_0 + 7_0 + 7_1$	$q_6 + q_7 + d_7$	332.3 MeV
s	$6_0 + 7_0 + 7_2$	$q_6 + q_7 + s_7$	558 MeV
c	$5_0 + 7_0 + 7_3$	$q_5 + q_7 + c_7$	1701 MeV
b	$6_0 + 7_0 + 7_4$	$q_6 + q_7 + b_7$	5318 MeV
t	$5_0 + 7_0 + 7_5 + 8_0 + 8_2$	$q_5 + q_7 + t_7 + q_8 + t_8$	176.5 GeV

3.4. The Lepton Formula

The principal dimensional fermion for heavy leptons (μ and τ) is e and ν_e. Auxiliary dimensional fermion is derived from principal dimensional boson in the same way as Eq. (32) to relate the energies for fermion and boson. For the mass of auxiliary dimensional fermion (AF) from principal dimensional boson (B), the equation is Eq. (37).

$$M_{AF_{d,a}} = \frac{M_{B_{d-1,0}}}{\alpha_a} \sum_{a=0}^{a} a^4 \quad , \tag{37}$$

where α_a = auxiliary dimensional fine structure constant, and a = auxiliary dimension number = 0 or integer. The first term, $\dfrac{M_{B_{D-1,0}}}{\alpha_a}$, of the mass formula (Eq.(37)) for the auxiliary dimensional fermions is derived from the mass equation, Eq. (32), for the principal dimensional fermions and bosons. The second term, $\sum\limits_{a=0}^{a} a^4$, of the mass formula is for Bohr-Sommerfeld quantization for a charge - dipole interaction in a circular orbit as described by A. Barut [36]. As in Barut lepton mass formula, $1/\alpha_a$ is 3/2. The coefficient, 3/2, is to convert the principal dimensional boson mass to the mass of the auxiliary dimensional fermion in the higher dimension by adding the boson mass to its fermion mass which is one-half of the boson mass. Using Eq. (32), Eq. (37) becomes the formula for the mass of auxiliary dimensional fermions (AF).

$$
\begin{aligned}
M_{AF_{d,a}} &= \frac{3M_{B_{d-1,0}}}{2}\sum_{a=0}^{a} a^4 \\
&= \frac{3M_{F_{d-1,0}}}{2\alpha_{d-1}}\sum_{a=0}^{a} a^4 \\
&= \frac{3}{2}M_{F_{d,0}}\alpha_d\sum_{a=0}^{a} a^4
\end{aligned}
\tag{38}
$$

The mass of this auxiliary dimensional fermion is added to the sum of masses from the corresponding principal dimensional fermions (F's) with the same electric charge or the same dimension. The corresponding principal dimensional leptons for u (2/3 charge) and d (-1/3 charge) are ν_e (0 charge) and e (-1 charge), respectively, by adding –2/3 charge to the charges of u and d [37]. The fermion mass formula for heavy leptons is derived as follows.

$$
M_{F_{d,a}} = \sum M_F + M_{AF_{d,a}}
$$

$$
= \sum M_F + \frac{3M_{B_{d-1,0}}}{2}\sum_{a=0}^{a} a^4
\tag{39a}
$$

$$
= \sum M_F + \frac{3M_{F_{d-1,0}}}{2\alpha_{d-1}}\sum_{a=0}^{a} a^4
\tag{39b}
$$

$$
= \sum M_F + \frac{3}{2}M_{F_{d,0}}\alpha_d\sum_{a=0}^{a} a^4
\tag{39c}
$$

Eq. (39b) is for the calculations of the masses of leptons. The principal dimensional fermion in the first term is e. Eq. (39b) can be rewritten as Eq. (40).

$$M_a = M_e + \frac{3M_e}{2\alpha} \, \overset{a}{\underset{a=0}{\Sigma}} a^4 , \qquad\qquad (40)$$

a = 0, 1, and 2 are for e, μ, and τ, respectively. It is identical to the Barut lepton mass formula.

3.5. The Quark Mass Formula

The auxiliary dimensional quarks except a part of t quark are q_7's. Eq.(39c) is used to calculate the masses of quarks. The principal dimensional quarks include $3\nu_\mu$, 3e, and 3μ., $\alpha_7 = \alpha_w$, and $q_7 = 3\mu$. Eq. (39c) can be rewritten as the quark mass formula.

$$M_q = \sum M_F + \frac{3\alpha_w M_{3\mu}}{2} \, \overset{a}{\underset{a=0}{\Sigma}} a^4 , \qquad\qquad (41)$$

where a = 1, 2, 3, 4, and 5 for u/d, s, c, b, and a part of t, respectively.

To match l_8 (ν_τ), quarks include q_8 as a part of t quark.   In the same way that $q_7 = 3\mu$, q_8 involves μ'. μ' is the sum of e, μ, and μ_8 (auxiliary dimensional lepton). Using Eq. (39a), the mass of μ_8 is equal to 3/2 of the mass of B_7, which is Z^0. Because there are only three families for leptons, μ' is the extra lepton, which is "hidden". μ' can appear only as μ + photon. The principal dimensional quark $q_8 = \mu'$ instead of 3μ', because μ' is hidden, and q_8 does not need to be 3μ' to be different. Using the equation similar to Eq.(41), the calculation for t quark involves $\alpha_8 = \alpha$, μ' instead of 3μ for principal fermion, and a = 1 and 2 for b_8 and t_8, respectively. The hiding of μ' for leptons is balanced by the hiding of b_8 for quarks.

The calculated masses are in good agreement with the observed constituent masses of leptons and quarks [38]. The mass of the top quark [39] is 174.3 ± 5.1 GeV in a good agreement with the calculated value, 176.5 GeV. All elementary particles (gauge bosons, leptons, and quarks) are in the periodic system of elementary particles with the calculated masses in good agreement with the observed values by using only four known constants: the number of the extra spatial dimensions in the eleven-dimensional membrane, the mass of electron, the mass of Z boson, and the fine structure constant.

With the masses of quarks calculated by the periodic table of elementary particles, the masses of all hardrons can be calculated [33] as the composes of quarks, as molecules are the composes of atoms. The calculated values are in good agreement with the observed values. For examples, the calculated masses of neutron and pion are 939.54MeV, and 135.01MeV in excellent agreement with the observed masses, 939.57 MeV and 134.98 MeV, respectively. At different temperatures, the strong force (QCD) among quarks in hadrons behaves differently to follow different dimensional orbitals [33].

3.6. The LHC Higgs Boson

The ATLAS and CMS experiments of CERN experiments observe a new particle in the mass region around 125-126 GeV with a high degree of certainty [40]. The decay modes and the spin of the new particle point to a Higgs boson.
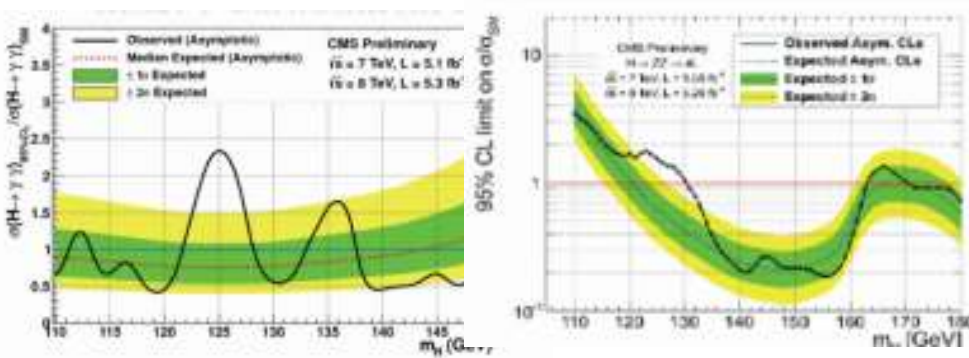
A deviation from the Standard Model is the excess decay rate to diphoton that was observed by both ATLAS and CMS as well as the Fermilab Tevatron [41]. The decay rate of diphoton is nearly twice as large as expected by the Standard Model. The significance of the discrepancy with the Standard Model is about 2.5 sigma. As long as this excess persists, it can be fitted by a non-standard (possibly negative) Yukawa couplings of the Higgs boson to the top quark, or explained by new charged boson contributions to the loop level process h → γγ. If that boson exists, it must have a mass larger than the W; otherwise, the Higgs would decay to this particle in pairs. Further work on diphoton is needed.

If the excess diphoton persists, it can be explained by the LHC Higgs boson. The LHC Higgs boson is the Higgs boson consisting of the SM Higgs boson and the hidden lepton condensate, similar to the top quark condensate [42] that is an alternative to the Higgs boson. The top quark condensate is a composite field composed of the top quark and its antiquark. The top quark condenses with its measured mass (173 GeV) comparable to the mass of the W and Z Bosons, so Vladimir Miransky, Masaharu Tanabashi, and Koichi Yamawaki proposed that the top quark condensate is responsible for the mass of the W and Z bosons. (As described later, the hidden leptons derived by the W boson and Z boson are partly responsible to the high mass of top quark.) The top quark condensate is analogous to Cooper pairs in a BCS superconductor and nucleons in the Nambu-Jona-Lasinio model. Anna Hasenfratz and Peter Hasenfratz et al. claimed that the top quark condensate is approximately equivalent to a Higgs scalar field. S. F. King proposed a tau lepton condensate to feed the tau mass to muon and electron [43].

Like the top quark condensate, the hidden lepton condensate is a composite field composed of the hidden leptons and its antileptons as μ', $\overline{\mu}$', μ'$^+$, and μ'$^-$. Like that the observed top quark is a bare quark with the observed mass of about 173 GeV instead of about 346 GeV for t $\overline{t}$, the observed hidden lepton is a bare average hidden lepton instead of μ' $\overline{\mu}$' and μ'$^+$ μ'$^-$. However, unlike the top quark condensate, the hidden lepton condensate is outside of the standard three lepton-quark families in the Standard Model. Being forbidden, a single hidden lepton cannot exist alone, so the hidden leptons must exist in the lepton condensate as the composite of the leptons-antileptons as μ', $\overline{\mu}$', μ'$^+$, and μ'$^-$. Being outside of the standard model family, the hidden lepton condensate decays into diphoton instead of leptons and quarks inside the standard model family.

The LHC Higgs boson consists of both the Higgs boson of the Standard Model and the adopted hidden lepton condensate. When the LHC Higgs boson decays, it decays as the Higgs boson of the Standard Model except the part of the adopted hidden lepton

condensate that decays into diphoton, resulting in the deviation in the rate of diphoton from the standard model. Other decay modes of the LHC Higgs boson follow the Standard Model (SM) as follows for the six decay modes of the LHC Higgs bosons.

The Decay Modes of the LHC Higgs boson

H (hidden lepton condensate) $\longrightarrow$ $\gamma\,\gamma$

H (SM) $\longrightarrow$ $\gamma\,\gamma$

H (SM) $\longrightarrow$ $Z\,Z$

H (SM) $\longrightarrow$ $W\,W$

H (SM) $\longrightarrow$ $b\,\bar{b}$

H (SM) $\longrightarrow$ $\tau\,\bar{\tau}$

The hidden leptons are derived from the periodic table of elementary particles that includes all elementary particles. Like the top quark condensate, the hidden lepton condensate is a composite field composed of the hidden leptons and its antileptons as μ', $\bar{\mu}'$, μ'^{+}, and μ'^{-} as in Table 3. To match l_8 (ν_τ), quarks include q_8 as a part of t quark. In the same way that $q_7 = 3\mu$, q_8 involves μ'. μ' is the sum of e, μ, and μ_8 (auxiliary dimensional lepton). Using Eq. (39a), the mass of μ_8 is equal to 3/2 of the mass of B_7, which is Z^0, and the mass of $\mu_8^{\pm}$ is equal to 3/2 of the mass of $B_7^{\pm}$, which is $W^{\pm}$.

$$\mu_8 = \frac{3}{2}Z^0$$

$$\mu' = 6_0 + 7_0 + 7_2 + 8_0 + 8_1 = \quad e + \nu_\mu + \mu_7 + \nu_\tau + \mu_8$$

$$\mu_8^{\pm} = \frac{3}{2}W^{\pm}$$

$$\mu'^{\pm} = 6_0 + 7_0 + 7_2 + 8_0 + 8_1^{\pm} = \quad e + \nu_\mu + \mu_7 + \nu_\tau + \mu_8^{\pm}$$

The calculated masses of the hidden lepton are 120.7 GeV (for the mass of $\mu'^{\pm}$) and 136.9 GeV (for the mass of μ') with the average as 128.8 GeV for the hidden lepton condensate in good agreements with the results from LHC (125 GeV or 126 GeV). The LHC Higgs boson acquires the mass of the hidden lepton condensate.

The Higgs boson is the scalar gauge boson to mediate the transformation between massive particle (mass) and massless particle (kinetic energy). The Higgs boson can be mass-giving or mass-removing. Before our universe, all particles were massive, the masses of all particles were equal, and our pre-universe was cold. At the beginning of our universe, the mass-removing Higgs boson converted massive particles into massless particles, resulting in the very hot universe to initiate the Big Bang. Afterward, the mass-giving Higgs boson converted some massless particles back to massive particles to differentiate dark matter and baryonic matter and to differentiate baryonic particles and forces with various

different masses. Without massless photon, dark matter is dark without electromagnetism, and incompatible (repulsive) to baryonic matter. The interactions of incompatible dark matter and baryonic matter generated the different shapes of galaxies. The baryonic particles and forces form the periodic table of elementary particles to calculate the masses of all elementary particles. Dark energy comes from the dark universe without the Higgs boson.

The Higgs boson itself is the gauge boson with zero mass-energy. The virtual Higgs boson is a property of space that can turn on the transformation between the massive particle (mass-potential energy) and massless particle (kinetic energy). (As described earlier, the transformation for different amounts of mass-energy is through another mechanism: the dimensional oscillation of object.) After the transformation, the Higgs boson remains dormant. With zero mass-energy, the Higgs boson avoids the severe problem of the huge energy (cosmological constant) from the gravity-Higgs boson interaction.

The observed LHC Higgs boson is a remnant of the Higgs boson, not the Higgs boson itself. The LHC Higgs boson is derived from the asymmetry (symmetry breaking) in the electroweak force consisting of the electromagnetic force with the massless gauge boson (photon) and the weak force with the massive gauge bosons (W+, W−, and Z). At the beginning of our universe, the coupling of the Higgs field and the electroweak force involved the four mass-giving Higgs bosons and the four gauge bosons (W+, W−, Z, and photon) in the electroweak force. The three Higgs bosons coupled with the three massless weak bosons (W+, W−, and Z), and were only observable as spin components of these weak bosons, which became massive; while the one remaining un-coupled Higgs boson became the residual unused Higgs boson after the transformation of the electroweak force. Since the transformation had finished, the residual unused Higgs boson could not remain zero mass-energy as the original Higgs boson, so it had to adopt a mass. The residual Higgs boson could not adopt any mass that already represented an independent elementary particle. The only available mass came from the hidden lepton in the form of the hidden lepton condensate. The electroweak, strong, and gravitational forces are separated forces, so there is no remnant of the Higgs boson from them.

3.7. Summary

For baryonic matter, the incorporation of detachment space for baryonic matter brings about "the dimensional orbitals" as the base for the periodic table of elementary particles for all leptons, quarks, and gauge bosons. The masses of gauge bosons, leptons, quarks can be calculated using only four known constants: the number of the extra spatial dimensions in the eleven-dimensional membrane, the mass of electron, the mass of $Z°$, and the fine structure constant. The calculated values are in good agreement with the observed values. The differences in dimensional orbitals result in incompatible dark matter and baryonic matter. The observed new LHC Higgs Boson consists of the SM (Standard Model) Higgs boson and the hidden lepton condensate that is in the forbidden lepton family outside of the standard three lepton families in the Standard Model. Being forbidden, a single hidden lepton cannot exist alone, so the hidden leptons must exist in the lepton condensate as the composite of the leptons-antileptons as μ', $\bar{\mu}'$, μ'^+, and μ'^-. The decay of the hidden lepton condensate into diphoton accounts for the observed excess diphoton deviated from the Standard Model. Other decay modes of the LHC Higgs boson follow

38

the Standard Model. The calculated masses of the hidden leptons of $\mu'^{\pm}$ and μ', are 120.7 GeV and 136.9 GeV, respectively, with the average as 128.8 GeV for the hidden lepton condensate in good agreements with the observed 125 or 126 GeV. The LHC Higgs boson acquires the mass of the hidden lepton condensate.

4. The Galaxy Formation

Introduction

The current observable universe contains dark energy, dark matter, and baryonic matter. As mentioned in the previous section, dark energy is from the dark universe to accelerate the expansion of the observable universe. Dark matter have different mass dimension from the baryonic matter. We live in the world of baryonic matter. The separation of baryonic matter and dark matter results in the galaxy formation.

4.1. The Separation of Baryonic Matter and Dark Matter

Dark matter has been detected only indirectly by means of its gravitational effects astronomically. Dark matter as weakly interacting massive particles (WIMPs) has not been detected directly on the earth [44]. The previous section proposes that the absence of the direct detection of dark matter on the earth is due to the incompatibility between baryonic matter and dark matter, analogous to incompatible water and oil. Chapter 2 provides the reasons for the incompatibility and the mass ratio (5 to 1) of dark matter to baryonic matter. Basically, during the inflation before the Big Bang, dark matter, baryonic matter, cosmic radiation, and the gauge force fields are generated. There are five types of dark matter with the "mass dimensions' from 5 to 9, while baryonic matter has the mass dimension of 4. As a result, the mass ratio is 5 to 1 as observed. Without electromagnetism, dark matter cannot emit light, and is incompatible to baryonic matter. Like oil, dark matter is completely non-polar. The common link between baryonic matter and dark matter is the cosmic radiation resulted from the annihilation of matter and antimatter from both baryonic matter and dark matter. The cosmic radiation is coupled strongly to baryonic matter through the electromagnetism, and weakly to dark matter without electromagnetism. With the high concentration of cosmic radiation at the beginning of the Big Bang, baryonic matter and dark matter are completely compatible. As the universe ages and expands, the concentration of cosmic concentration decreases, resulting in the increasing incompatibility between baryonic matter and dark matter until the incompatibility reaches to the maximum value with low concentration of cosmic radiation.

The incompatibility is expressed in the form of the repulsive MOND (modified Newtonian dynamics) force field. MOND [45] proposes the deviation from the Newtonian dynamics in the low acceleration region in the outer region of a galaxy. This paper proposes the MOND forces in the interface between the baryonic matter region and the dark matter region [46]. In the interface, the same matter materials attract as the conventional attractive MOND force, and the different matter materials repulse as the repulsive MOND force between baryonic matter and dark matter.

Baryonic matter region (Newtonian regime)

Interface (MOND regime)
$a_i \ll a_0$, $a_i = (a_N a_0)^{1/2}$

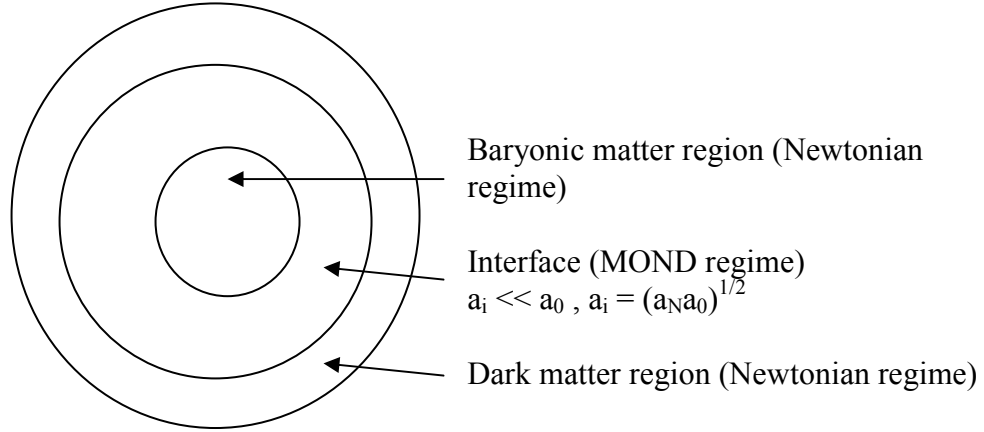Dark matter region (Newtonian regime)

Figure 9: the interfacial region between the baryonic and the dark matter regions

In Figure 9, the inner part is the baryonic matter region, the middle part is the interface, and the outer part is the dark matter region. The MOND forces in the interface are the interfacial attractive force (conventional MOND force), $F_{i\text{-}A}$, among the same matter materials and the interfacial repulsive force (repulsive MOND force), $F_{i\text{-}R}$, between baryonic matter material and dark matter material. The interfacial repulsive force enhances the interfacial attractive force toward the center of gravity in terms of the interfacial acceleration, a_i.

The border between the baryonic matter region and the interface is defined by the acceleration constant, a_0. The interfacial acceleration is less than a_0. The enhancement is expressed as the square root of the product of a_i and a_0. In the baryonic matter region, a_b is greater than a_0, and is equal to normal Newtonian acceleration as Eq. (42).

$$a_0 \ll a_b, \quad a_b = a_N \ \text{in the baryonic matter region}$$
$$a_0 \gg a_i, \quad a_i = \sqrt{a_N a_0} \ \text{in the int} \, erfacial \ region \tag{42}$$

The interfacial attractive force in the interface with the baryonic matter region is expressed as Eq. (43) where m is the mass of baryonic material in the interface.

$$F_{i-A} = ma_N$$
$$= m \frac{a_i^{\,2}}{a_O} , \tag{43}$$

The comparison of the interfacial attractive force, $F_{i\text{-}A}$, and the non-existing interfacial Newtonian attractive force, $F_{i\text{-Newton}}$ in the interface is as Eqs. (44), (45), and (46), where G is the gravitation constant, M is the mass of the baryonic material, and r the distance between the gravitational center and the material in the infacial region.

$$F_{i-A} = \frac{GMm}{r^2}$$

$$= m\frac{a^2}{a_0},$$

$$F_{i-Newton} = \frac{GMm}{r^2}$$

$$= m\,a \tag{44}$$

$$a_i = \frac{\sqrt{GMa_0}}{r}$$

$$a_{i-Newron} = \frac{GM}{r^2}, \tag{45}$$

$$F_{i-A} = \frac{m\sqrt{GMa_0}}{r}$$

$$F_{i-Newron} = \frac{mGM}{r^2}, \tag{46}$$

The interfacial attractive force decays with r, while the interfacial Newtonian force decays with r^2. Therefore, in the interface when $a_0 \gg a_i$, with sufficient dark matter, the interfacial repulsive force, F_{i-R}, is the difference between the interfacial attractive force and the interfacial Newtonian force as Eq. (47).

$$a_0 \gg a_i, \text{ in the } int\!erfacial \ \ region$$

$$F_{i-R} = F_{i-A} - F_{i-Newton} \tag{47}$$

$$= m\left(\frac{\sqrt{GMa_0}}{r} - \frac{GM}{r^2}\right)$$

The same interfacial attractive force and the interfacial repulsive force also occur for dark matter in the opposite direction. Thus, the repulsive MOND force filed results in the separation of baryonic matter and dark matter.

The acceleration constant, a_0, represents the maximum acceleration constant for the maximum incompatibility between baryonic matter and dark matter. The common link between baryonic matter and dark matter is cosmic radiation resulted from the annihilation of matter and antimatter from both baryonic matter and dark matter. With the high concentration of cosmic radiation at the Big Bang, baryonic matter and dark matter are completely compatible. As the universe ages and expands, the concentration of cosmic concentration decreases, resulting in the increasing incompatibility between baryonic matter and dark matter. The incompatibility reaches maximum when the concentration of cosmic radiation becomes is too low for the compatibility between baryonic matter and dark matter. Therefore, for the early universe before the formation of galaxy when the concentration of cosmic radiation is still high, the time-dependent Eq. (42) is as Eq. (48).

$$a_i = \sqrt{\frac{a_N a_0 t}{t_0}} \ \ for \ t_0 \geq t \ , \qquad (48)$$

where t is the age of the universe, and t_0 is the age of the universe to reach the maximum incompatibility between baryonic matter and dark matter.

The distance, r_0, from the center to the border of the interface is as Eq. (49).

$$r_0 \qquad = \qquad \sqrt{GM/a_0} \qquad\qquad (49)$$

In the early universe, r_0 decreases with the age of the universe as Eq. (50).

$$r_0 \qquad = \qquad \sqrt{\frac{GMt_0}{a_0 t}} \qquad\qquad (50)$$

The decreases in r_0 leads to the increase in the interface where the interfacial forces exist. The interfacial forces also increase with time.

$$a_0 \gg a_i \, , in \ the \ \mathrm{int}erfacial \ \ region$$
$$F_{i-R} = F_{i-A} \ - \ F_{i-Newton} \qquad\qquad (51)$$
$$= m\,(\frac{\sqrt{GMa_0 t/t_0}}{r} \ - \ \frac{GM}{r^2})$$

To minimize the interface and the interfacial forces, the same matter materials increasingly come together to form the matter droplets separating from the different matter materials. The increasing formation of the matter droplets with increasing incompatibility is similar to the increasing formation of oil droplets with increasing incompatibility between oil and water. Since there are more dark matter materials than baryonic matter materials, most of the matter droplets are baryonic droplets surrounded by dark matter materials. The early universe is characterized by the increases in the size and the number of the matter droplets due to the increasing incompatibility between baryonic matter and dark matter.

4.2. The Formation of the Inhomogeneous Structures

The Inflationary Universe scenario [47] provides possible solutions of the horizon, flatness and formation of structure problems. In the standard inflation theory, quantum fluctuations during the inflation are stretched exponentially so that they can become the seeds for the formation of inhomogeneous structure such as galaxies and galaxy clusters.

This paper posits that the inhomogeneous structure comes from both quantum fluctuation during the inflation and the repulsive MOND force between baryonic matter

and dark matter after the inflation. As mentioned in the previous section, the increasing repulsive MOND force field with the increasing incompatibility in the early universe results in the increase in the size and number of the matter droplets.

For the first few hundred thousand years after the Big Bang (which took place about 13.7 billion years ago), the universe was a hot, murky mess, with no light radiating out. Because there is no residual light from that early epoch, scientists can't observe any traces of it. But about 400,000 years after the Big Bang, temperatures in the universe cooled, electrons and protons joined to form neutral hydrogen as the recombination. The inhomogeneous structure as the baryonic droplets by the incompatibility between baryonic matter and dark matter is observed [48] as anisotropies in CMB (cosmic microwave background).

As the universe expanded after the time of recombination, the density of cosmic radiation decreases, and the size of the baryonic droplets increased with the increasing incompatibility between baryonic matter and dark matter. The growth of the baryonic droplet by the increasing incompatibility from the cosmic expansion coincided with the growth of the baryonic droplet by gravitational instability from the cosmic expansion. The formation of galaxies is through both gravitational instability and the incompatibility between baryonic matter and dark matter.

The pre-galactic universe consisted of the growing baryonic droplets surrounded by the dark matter halos, which connected among one another in the form of filaments and voids. These dark matter domains later became the dark matter halos, and the baryonic droplets became galaxies, clusters, and superclusters.

When there were many baryonic droplets, the merger among the baryonic droplets became another mechanism to increase the droplet size and mass. When three or more homogeneous baryonic droplets merged together, dark matter was likely trapped in the merged droplet (C, D, E, and F in Fig. 10). The droplet with trapped dark matter inside is the heterogeneous baryonic droplet, while the droplet without trapped dark matter inside is the homogeneous baryonic droplet.
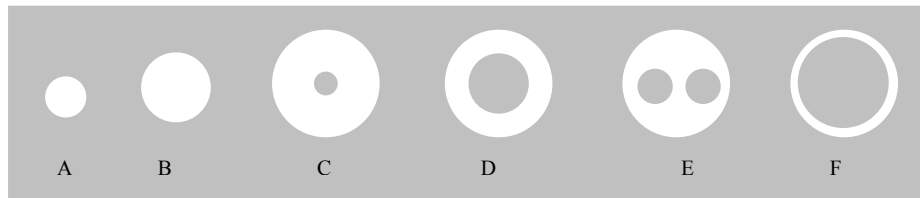

Fig. 10: the homogeneous baryonic droplets (A, and B), and the heterogeneous baryonic droplets (C, D, E, and F)

In the heterogeneous droplets C, D, E, and F, dark matter was trapped in the cores of the baryonic droplets. Because of the prevalence of dark matter, almost all baryonic droplets were the heterogeneous droplets. There were the dark matter core, the baryonic matter shell, and the dark matter halo around the baryonic droplet, resulting in two repulsive forces as the pressures between the dark matter core and the baryonic matter shell and between the baryonic shell and the dark matter halo. In the equilibrium state, the internal pressure between the dark matter core and the baryonic matter shell was same as the external pressure between the baryonic shell and the dark matter halo.

When the temperature dropped to ~ 1000°K, some hydrogen atoms in the droplet paired up to create the primordial molecular layers. Molecular hydrogen cooled the primordial molecular layers by emitting infrared radiation after collision with atomic hydrogen. Eventually, the temperature of the molecular layers dropped to around 200 to 300°K, reducing the gas pressure and allowing the molecular layers to continue contracting into gravitationally bound dense primordial molecular clouds. The diameters of the primordial could be up to 100 light-years with the masses of up to 6 million solar masses. Most of baryonic droplets contained thousands of the primordial molecular clouds.

The formation of the primordial molecular clouds created the gap in the baryonic matter shell. The gap allowed the dark matter in the dark matter core to leak out, resulting in a tunnel between the dark matter core and the external dark matter halo. The continuous leaking of the dark matter expanded the tunnel. Consequently, the dark matter in the dark matter core rushed out of the dark matter core, resulting in the "Big Eruption". The ejection of the dark matter from the dark matter core reduced the internal pressure between the dark matter core and the baryonic matter shell. The external pressure between the baryonic matter shell and the dark matter halo caused the collapse of the baryonic droplet. The collapse of the baryonic droplet is like the collapse of a balloon as the air (as dark matter) moves out the balloon.

The collapse of the baryonic droplet forced the head-on collisions of the primordial molecular clouds in the baryonic matter shell. In the center of the collapsed baryonic droplet, the head-on collisions of the primordial molecular clouds generated the shock wave as the turbulence in the collided primordial molecular clouds. The turbulence triggered the collapse of the core of the primordial cloud. The core fragmented into multiple stellar embryos, in each a protostar nucleated and pulled in gas. Without the heavy elements to dissipate heat, the mass of the primordial protostar was 500 to 1,000 solar masses at about 200°K. The primordial protostar shrank in size, increased in density, and became the primordial massive star when nuclear fusion began in its core. The massive primordial star formation is as follows.

$$incompatible\ dark\ matter\ and\ baryonic\ matter \longrightarrow homogeneous\ baryonic\ droplets \xrightarrow{combination} heterogeneous$$

$$baryonic\ droplet \xrightarrow{the\ cooling} molecular\ clouds\ in\ baryonic\ matter\ shell \xrightarrow{eruption,\ collapse,\ and\ collision}$$

$$protostar \xrightarrow{nuclear\ fusion} massive\ primordial\ star$$

The intense UV radiation from the high surface temperature of the massive primordial stars started the reionization effectively, and also triggered further star formation. The massive primordial stars were short-lived (few million years old). The explosion of the massive primordial stars was the massive supernova that caused reionization and triggered star formation. The heavy elements generated during the primordial star formation scattered throughout the space. The dissipation of heat by heavy elements allowed the normal rather than massive star formation. With many ways to trigger star formation, the rate of star formation increased rapidly. The Big Eruption that initiated the star formation started to occur about 400 million years after the Big Bang, and the reionization started to occur soon after. The rate of star formation peaked about 2 billion years after the Big Bang [49].

Since the head-on collision of the molecular clouds took place at the center of the collapsed baryonic droplet, the star formation started in the center of the collapsed

baryonic droplet.   With other ways to trigger star formation, the star formation propagated away from the center. The star formation started from the center from which the star formation propagated, so the primordial galaxies appeared to be small surrounded by the large hydrogen blobs. The surrounding large hydrogen blobs corresponds to the observed Lyman alpha blobs of Lyman alpha (Lya) emission by hydrogen, which have been discovered in the vicinity of galaxies at early cosmic times. The amount of hydrogen in the blobs was also increased by the incoming abundant intergalactic hydrogen.   The repulsive dark matter halos prevented the hydrogen gas inside from escaping from the galaxies. Dijkstra and Loeb [50] posited that the early galaxies grew quickly by the cold accretion mode from the observed Lyman alpha blobs.   The growth by the merger of galaxies was too slow for the observed fast growth of the early galaxies.

If there was small dark matter core as in the heterogeneous baryonic droplet (C in Figure 10), the Big Eruption took relatively short time to cause the collapse of the baryonic droplet. The change in the shape of the baryonic droplet after the collapse was relatively minor. The collapse results in elliptical shape in E_0 to E_7 elliptical galaxies, whose lengths of major axes are proportional to the relative sizes of the dark matter core. Because of the short time for the collapse of the baryonic droplet, the star formation by the collapse occurred quickly at the center.
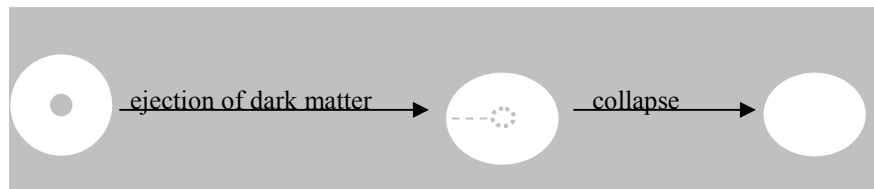
Most of the primordial stars merged to form the supermassive center, resulting in the quasar galaxies. Such first quasar galaxies that occurred as early as z = 6.28 were observed to have about the same sizes as the Milky Way [51]. This formation of galaxy follows the monolithic collapse model in which baryonic gas in galaxies collapses to form stars within a very short period, so there are small numbers of observed young stars in elliptical galaxies. Elliptical galaxies continue to grow slowly as the universe expands.

If the size of the dark matter core is medium (D in Fig. 10), the collapse of the baryonic droplet caused a large change in shape, resulting in the rapidly rotating disk as spiral galaxy. The rapidly rotating disk underwent differential rotation with the increasing angular speeds toward the center. After few rotations, the structure consisted of a bungle was formed and the attached spiral arms as spiral galaxy as Fig. 11.
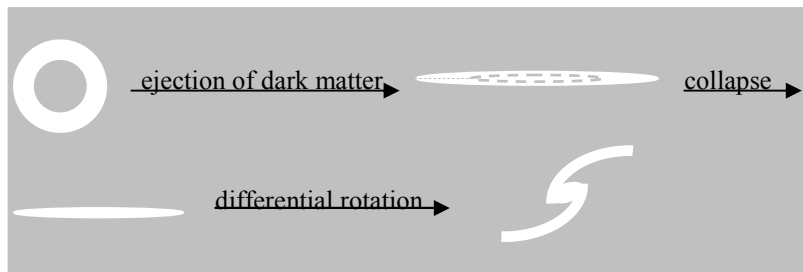

Fig. 11: the formation of spiral galaxy

The spiral galaxy took longer time to erupt and collapse than the elliptical galaxy, so the star formation was later than elliptical galaxy. Because of the large size of the dark matter core, the density of the primordial molecular clouds was lower than elliptical galaxy, so the rate of star formation in spiral galaxy is slower than elliptical galaxy. During the collapse of the baryonic droplet, some primordial molecular clouds moved away to form globular clusters near the main group of the primordial molecular clouds. Most of the primordial massive stars merged to form the supermassive center. The merge of spiral galaxies with comparable sizes destroys the disk shape, so most spiral galaxies are not merged galaxies.

When two dark matter cores inside far apart from each other (E in Fig. 10) generated two openings in opposite sides of the droplet, the dark matter could eject from both openings. The two opening is equivalent to the overlapping of two ellipses, resulting in the thick middle part, resulting in the star formation in the thick middle part and the formation of barred spiral galaxy. The differential rotation is similar to that of spiral galaxy as Fig. 12.
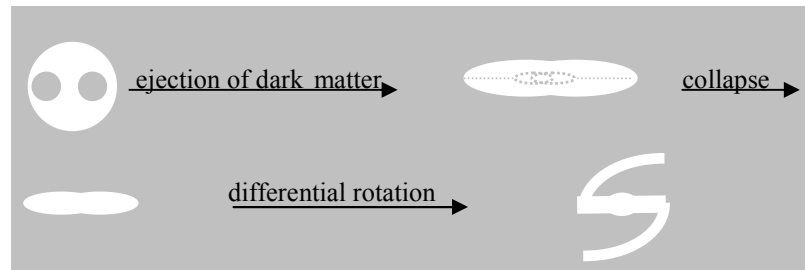

Fig. 12: the formation of barred spiral galaxy

As in normal spiral galaxy, the length of the spiral arm depends on the size of the dark matter core. The smallest dark matter core for barred spiral galaxy brings about SBa, and the largest dark matter core brings about SBd. The stars form in the low-density spiral arms much later than in the nucleus, so they are many young stars in the spiral arms. In barred spiral galaxy, because of the larger dark matter core area than normal spiral galaxy, the star formation occurred later than normal spiral galaxy, and the rate of star formation was slower than normal spiral galaxy.

If the size of the dark matter core was large (F in Fig. 10), the eruption of the dark matter in the dark matter core occurred easily in multiple places. The baryonic matter shell became fragmented, resulting in irregular galaxy. The turbulence from the collapse of the baryonic droplet was weak, and the density of the primordial molecular clouds was low, so the rate of star formation was slow. The star formation continues in a slow rate up to the present time.

At the end of the Big Eruption, vast majority of baryonic matter was primordial free baryonic matter resided in dark matter outside of the galaxies from the Big Eruption. This free baryonic matter constituted the intergalactic medium (IGM). Stellar winds, supernova winds, and quasars provide heat and heavy elements to the IGM as ionized baryonic atoms. The heat prevented the formation of the baryonic droplet in the IGM.

Galaxies merged into new large galaxies, such as giant elliptical galaxy and cD galaxy (z > 1-2). Similar to the transient molecular cloud formation from the ISM (inter-stellar medium) through turbulence, the tidal debris and turbulence from the mergers generated the numerous transient molecular regions, which located in a broad area [52].

The incompatibility between baryonic matter and dark matter transformed these transient molecular regions into the stable second-generation baryonic droplets surrounded by the dark matter halos. The baryonic droplets had much higher fraction of hydrogen molecules, much lower fraction of dark matter, higher density, and lower temperature, and lower entropy than the surrounding.

During this period, the acceleration constant reached to the maximum value with the maximum incompatibility between baryonic matter and dark matter. The growth of the baryonic droplets did not depend on the increasing incompatibility. The growth of the baryonic droplets depended on the turbulences that carried IGM to the baryonic droplets. The rapid growth of the baryonic droplets drew large amount of the surrounding IGM inward, generating the IGM flow shown as the cooling flow. The IGM flow induced the galaxy flow. The IGM flow and the galaxy flow moved toward the merged galaxies, resulting in the protocluster (z ~ 0.5) with the merged galaxies as the cluster center.

Before the protocluster stage, spirals grew normally and passively by absorbing gas from the IGM as the universe expanded. During the protoculster stage (z ~ 0.5), the massive IGM flow injected a large amount of gas into the spirals that joined in the galaxy flow. Most of the injected hot gas passed through the spiral arms and settled in the bungle parts of the spirals. Such surges of gas absorption from the IGM flow resulted in major starbursts (z ~ 0.4) [53]. Meanwhile, the nearby baryonic droplets continued to draw the IGM, and the IGM flow and the galaxy flow continued. The results were the formation of high-density region, where the galaxies and the baryonic droplets competed for the IGM as the gas reservoir. Eventually, the maturity of the baryonic droplets caused a decrease in drawing the IGM inward, resulting in the slow IGM flow. Subsequently, the depleted gas reservoir could not support the major starbursts (z ~ 0.3). The galaxy harassment and the mergers in this high-density region disrupted the spiral arms of spirals, resulting in S0 galaxies with indistinct spiral arms (z ~ 0.1 − 0.25). The transformation process of spirals into S0 galaxies started at the core first, and moved to the outside of the core. Thus, the fraction of spirals decreases with decreasing distance from the cluster center.

The static and slow-moving second-generation baryonic droplets turned into dwarf elliptical galaxies and globular clusters. The fast moving second-generation baryonic droplets formed the second-generation baryonic stream, which underwent a differential rotation to minimize the interfacial area between the baryonic matter and dark matter. The result is the formation of blue compact dwarf galaxies (BCD), such as NGC 2915 with very extended spiral arms. Since the star formation is steady and slow, so the stars formed in BCD are new.

The galaxies formed during z < 0.1-0.2 are mostly metal-rich tidal dwarf galaxies (TDG) from tidal tails torn out from interacting galaxies. In some cases, the tidal tail and the baryonic droplet merge to generate the starbursts with higher fraction of molecule than the TDG formed by tidal tail alone [54].

When the interactions among large galaxies were mild, the mild turbulence caused the formation of few molecular regions, which located in narrow area close to the large galaxies. Such few molecular regions resulted in few baryonic droplets, producing weak IGM flow and galaxy flow. The result is the formation of galaxy group, such as the Local Group, which has fewer dwarf galaxies and lower density environment than cluster.

Clusters merged to generate tidal debris and turbulence, producing the baryonic droplets, the ICM (intra-cluster medium) flow, and the cluster flow. The ICM flow and the cluster flow directed toward the merger areas among clusters and particularly the rich clusters with high numbers of galaxies. The ICM flow is shown as the warm filaments outside of cluster [55]. The dominant structural elements in superclusters are single or multi-branching filaments [56]. The cluster flow is shown by the tendency of the major axes of clusters to point toward neighboring clusters [57]. Eventually, the observable expanding universe will consist of giant voids and superclusters surrounded by the dark matter halos.

In summary, the whole observable expanding universe is as one unit of emulsion with incompatibility between baryonic matter and dark matter. The five periods of baryonic structure development are the free baryonic matter, the baryonic droplet, the galaxy, cluster, and the supercluster periods as Fig. 13. The first-generation galaxies are elliptical, normal spiral, barred spiral, and irregular galaxies. The second-generation galaxies are giant ellipticals, cD, evolved S0, dwarf ellipticals, BCD, and TDG. The universe now is in the early part of the supercluster period.
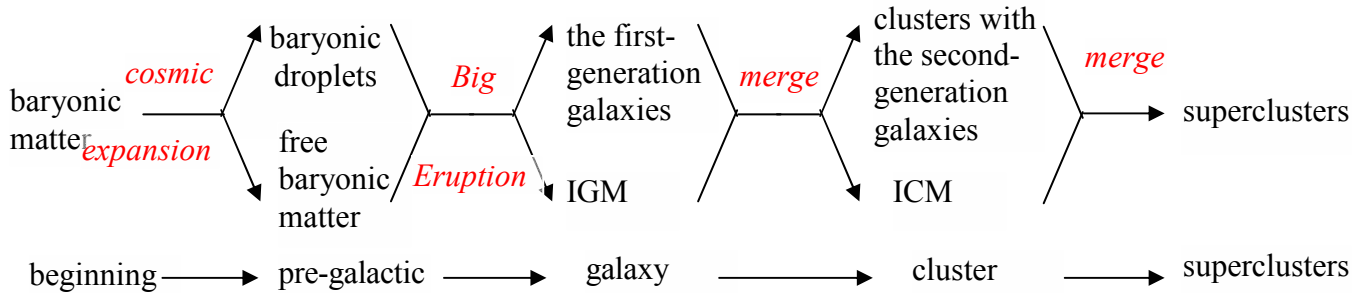

Fig. 13: the five levels of baryonic structure in the universe

4.3. Summary

The separation of dark matter without electromagnetism and baryonic matter with electromagnetism involves MOND (modified Newtonian dynamics). It is proposed that the MOND force is in the interface between the baryonic matter region and the dark matter region. In the interface, the same matter materials attract as the conventional attractive MOND force, and the different matter materials repulse as the repulsive MOND force between baryonic matter and dark matter. The source of the repulsive MOND force field is the incompatibility between baryonic matter and dark matter, like water and oil. The incompatibility does not allow the direct detection of dark matter. Typically, dark matter halo surrounds baryonic galaxy. The repulsive MOND force between baryonic matter and dark matter enhances the attractive MOND force of baryonic matter in the interface toward the center of gravity of baryonic matter. The enhancement of the low acceleration in the interface is by the acceleration constant, a_0, which defines the border of the interface and the factor of the enhancement. The enhancement of the low gravity in the interface is by the decrease of gravity with the distant rather than the square of distance as in the normal Newtonian gravity. The repulsive MOND force is the difference between the attractive MOND force and the non-

existing interfacial Newtonian force. The repulsive MOND force field results in the separation and the repulsive force between baryonic matter and dark matter.

The repulsive MOND force field explains the evolution of the inhomogeneous baryonic structures in the universe. Both baryonic matter and dark matter are compatible with cosmic radiation, so in the early universe, the incompatibility between baryonic matter and dark matter increases with decreasing cosmic radiation and the increasing age of the universe until reaching the maximum incompatibility. The repulsive MOND force field with the increasing incompatibility results in the growth of the baryonic matter droplets. The five stages of the formation of inhomogeneous structures are baryonic matter, baryonic droplets, the first generation galaxies by the Big Eruption, cluster, and supercluster.

The three periods for the baryonic structure development in the early universe are the free baryonic matter, the baryonic droplet, and the galaxy formation from the Big Eruption. The transition to the baryonic droplet generates density perturbation in the CMB. In the galaxy period, the first-generation galaxies including elliptical, normal spiral, barred spiral, and irregular galaxies were the result of the Big Eruption from the inhomogeneous baryonic droplets.

After reaching the maximum incompatibility, the growth of the baryonic droplets depends on the turbulence, resulting in the baryonic structure development of the cluster and the supercluster. In the cluster period, the second-generation galaxies include modified giant ellipticals, cD, evolved S0, dwarf elliptical, BCD, and tidal dwarf galaxies. The whole observable expanding universe behaves as one unit of emulsion with incompatibility between baryonic matter and dark matter through the repulsive MOND force field.

5. The Extreme Force Field

5.1. The quantum space phase transitions for force fields

Under extreme conditions such as the absolute zero temperature or extremely high pressure, binary lattice space for a gauge force field undergoes a phase transition to become binary partition space for the extreme force fields [5] [7].

At zero temperature or extremely high pressure, binary lattice space for a gauge force field undergoes a quantum space phase transition to become binary partition space. In binary partition space, detachment space and attachment space are in two separate continuous regions as follows.

$$\left(1_4\right)_m + \sum_{k=1}^{k} \left(\left(0_4\right)\left(1_4\right)\right)_{n,k} \longrightarrow \left(1_4\right)_m + \sum_{k=1}^{k} \left(0_4\right)_{n,k} \left(1_4\right)_{n,k}$$

$$\begin{matrix} particle \quad boson \quad field & extreme \quad particle \quad extreme \; boson \; field \\ in \; binary \; lattice \; space & in \; binary \; partition \; space \end{matrix} \qquad (52)$$

The force field in binary lattice space is gauge boson force field, the force field in binary partition space is denoted as "extreme boson force field". The detachment space in extreme boson field is the vacuum core, while extreme bosons attached to attachment space form the extreme boson shell. Gauge boson force field has no boundary, while the attachment space in the binary partition space acts as the boundary for extreme boson force field. Extreme boson field is like a bubble with core vacuum surrounded by membrane where extreme bosons locate.

The overlapping (connection) of two extreme bosons from two different sites results in "extreme bond". The product is "extreme molecule". An example of extreme molecule is Cooper pair, consisting of two electrons linked by extreme bond. Another example is superfluid, consisting of molecules linked by extreme bonds. Extreme bonds can be also formed among the sites in a lattice, resulting in extreme lattice. Extreme lattice is superconductor. Extreme boson force is incompatible to gauge boson force field. The incompatibility of extreme boson force field and gauge boson force field manifests in the Meissner effect, where superconductor (extreme lattice) repels external magnetism. The energy (stiffness) of extreme boson force field can be determined by the penetration of boson force field into extreme boson force field as expressed by the London equation for the Meissner effect.

$$\nabla^2 H = -\lambda^{-2} H \quad , \qquad (53)$$

where H is an external boson field and λ is the depth of the penetration of magnetism into extreme boson shell. This equation indicates that the external boson field decays exponentially as it penetrate into extreme boson force field.

5.2. Superconductor and the Fractional Quantum Hall Effect

Extreme boson exists only at the absolute zero temperature. However, quantum fluctuation at a temperature close to zero temperature allows the formation of an extreme boson. The temperature is the critical temperature (T_c). Such temperature constitutes the quantum critical point (QCP) [58]. Extreme boson at QCP is the base of superconductivity.

The standard theory for the conventional low temperature conductivity is the BCS theory. According to the theory, as one negatively charged electron passes by the positively charged ions in the lattice of the superconductor, the lattice distorts. This in turn causes phonons to be emitted which forms a channel of positive charges around the electron. The second electron is drawn into the channel. Two electrons link up to form the "Cooper pair" without the normal repulsion.

In the extreme boson model of the BCS theory, an extreme boson instead of a positive charged phonon is the link for the Cooper pair. According the extreme boson model, as an electron passes the lattice of superconductor, lattice atom absorbs the energy of the passing electron to cause a lattice bond to stretch or to contract. When the lattice bond recoils to normal position, the lattice atom emits a phonon, which is absorbed by the electron. The electron then emits the phonon, which is absorbed by the next lattice atom to cause its bond to stretch. When the lattice bond recoils to normal position, the lattice atom emits a phonon, which is absorbed by the electron. The result is the continuous lattice vibration by the exchanges of phonons between the electrons in electric current and the lattice atoms in lattice.

At the temperature close to the absolute zero temperature, the lattice vibration continuously produces phonons, and through quantum fluctuation, a certain proportion of phonons converts to extreme bosons. Extreme bonds are formed among extreme bosons, resulting in extreme lattice. At the same time, the electrons involved in lattice vibration form extreme molecules as Cooper pairs linked by extreme bonds. Such extreme bond excludes electromagnetism, including the Coulomb repulsive force, between the two electrons. When Cooper pairs travel along the uninterrupted extreme bonds of an extreme lattice, Cooper pairs experience no resistance by electromagnetism, resulting in zero electric resistance. Extreme lattice repels external magnetism as in the Meissner effect.

The extreme bosons involved in the formation of the extreme lattice bonds and the extreme molecular bonds have the energy, so the extreme bond energy (E_l) for the extreme lattice is same as the extreme bond energy (E_c) for Cooper pair.

$$E_l = E_c$$
$$= 2\Delta_0$$

(54)

The extreme bond energy corresponds to two times the energy gap Δ_t at zero temperature in the BCS theory. The energy gap is the superconducting energy that an electron has. Δ_t approaches to zero continuously as temperature approaches to T_c. The elimination of superconductivity is to break the extreme bonds of the extreme lattice and Cooper pairs.

Extreme boson force is a confined short distant force, so the neighboring extreme bosons have to be close together. To have a continuous extreme lattice without gaps, it is necessary to have sufficient density of the vibrating lattice atoms. Thus, there is critical

density, D_c, of vibrating lattice atoms. Below D_c, no extreme lattice can be formed. In a good conductor, an electron hardly interacts with lattice atoms to generate lattice vibration for extreme boson, so a good conductor whose density for vibrating lattice atoms below D_c does not become a superconductor. T_c is directly proportional to the density of vibrating lattice atoms and the frequency of the vibration (related to the isotope mass).

The "gap" in extreme lattice is the area without vibrating lattice atoms. The gap allows electric resistance. Superconductor has "perfect extreme lattice" without significant gap, while "imperfect extreme lattice" has significant gap to prevent the occurrence of superconductivity.

High temperature superconductor has a much higher T_c than low temperature superconductor described by the BCS theory. All high temperature superconductors involve the particular type of insulator with various kinds of dopants. A typical insulator is Mott insulator, such as copper oxides, CuO_2. CuO_2 forms a two-dimensional layer, with the Cu atoms forming a square lattice and O atoms between each nearest-neighbor pair of Cu atoms. In the undoped CuO_2, all of the planar coppers are in the Cu2+ state, with one unpaired electron per site. Two neighboring unpaired electrons with antiparallel spins have lower ground energy than two neighboring unpaired electrons with parallel spins. Two neighboring unpaired electrons with antiparallel spins constitute the antiparallel spin pair, which has lower ground state energy than the parallel spin pair. Consequently, CuO_2 layer consists of the antiparallel spin pairs, resulting in antiferromagnetism.

The insulating character of this state is thought to result, not from the antiferromagnetism directly, but from the strong on-site Coulomb repulsion, which is the energy cost of putting an extra electron on a Cu atom to make Cu^{1+}. This Coulomb energy for double occupancy suppresses conduction.

$La_x Sr_x Cu_2 O_4$ is an example of high temperature conductor. The key ingredient consists of CuO_2 layers. The doping of Sr provides chemical environment to shift the charge away from the CuO_2 layers, leaving "doping holes" in the CuO_2 layers. The shifting of electrons allows the occurrence of electric current. In the t-J model of high temperature superconductor, an electron in electric current is fractionalized into two fractional electrons to carry spin quantum number in t and to carry charge in J [59].

$$H_{ij} = -t\sum_{ij\sigma} \widetilde{c}_{i\sigma}^{+} \widetilde{c}_{j\sigma} + J\sum_{ij}\left[\vec{S}_i \bullet \vec{S}_j - \frac{n_i n_j}{4} \right] \, , \qquad (55)$$

In the extreme boson model, t corresponds to the spin current (spinon) to generate spin fluctuation in the metal oxide layer, while J corresponds to the directional charge current (phonon as in the BCS theory) along the metal oxide layers. Extreme boson force field is a confined force field. As long as electrons are in the confined extreme boson force field, it is possible to have fractioanlized electrons, similar to the fractionalized charges of quarks in the gluon force field.

The spin fluctuation generated by the spin current in the layer comes from doping holes in CuO_2 layer. When an antiparallel spin pair loses an electron by doping, a doping

hole is in the spin pair. The adjacent electron outside of the pair fills in the hole. The filled-in electron has a parallel spin as the electron in the original pair. Parallel spin pair has higher ground state energy than antiparallel pair, so the filled-in electron absorbs a spinon to gain enough energy to undergo a spin change. The result is the formation of an antiparallel spin pair. The antiparallel spin pair has lower ground state energy than an antiparallel spin pair, so it emits a spinon. After the electron fills the hole, the hole passes to the next adjacent pair. The next adjacent pair then becomes the next adjacent newly formed parallel pair, which then absorbed the emitted spinon undergo spin change to form an antiparallel spin pair. The continuous passing of holes constitutes the layer spin current. The layer spin current throughout the CuO_2 layer generates the continuous spin fluctuation [60] with continuous emission and absorption of spinons.

At a low temperature, the spin fluctuation continuously produces spinons, and through quantum fluctuation, a certain proportion of spinons converts to extreme bosons. Extreme bonds are formed among extreme bosons. The extreme bonds are the parallel extreme bonds parallel to CuO_2 layer. The parallel extreme bond results from the spin current.

The extreme bonds connecting CuO_2 layers are the perpendicular bonds perpendicular to CuO_2 layers through d-wave by the lattice vibration, like the lattice vibration in the low temperature superconductor. The perpendicular bond results from the charge current. The perpendicular extreme bond energy ($E_\perp$) is greater than the parallel extreme bond energy (E_{II}). Cooper pairs as the charge pairs travel along the perpendicular bonds. Thus, Cooper pair has the same bond as the perpendicular extreme bond. The extreme lattice consists of both parallel extreme bonds and perpendicular extreme bonds.

$$E_{II} < E_\perp$$
$$E_c = E_\perp \quad , \qquad (56)$$
$$E_l = E_{II, \perp}$$

Perfect extreme lattice without gap of extreme bonds consists of both perfect parallel extreme lattice and perfect perpendicular extreme lattice without gaps for parallel extreme bonds and perpendicular bonds, respectively. The T_c of high temperature superconductor the transition temperature to the perfect extreme lattice, consisting of the perfect parallel extreme lattice and the perfect perpendicular lattice. Because many extreme bosons are generated from many spin fluctuations, T_c is high.

Having stronger extreme bond, the $T_{c\,\perp}$ for the perpendicular extreme lattice is higher than the $T_{c\,II}$ for the parallel extreme lattice. Thus, T_c for the extreme lattice is essentially the $T_{c\,II}$ for the parallel extreme lattice.

$$T_{c\,II} < T_{c\,\perp}$$
$$T_c = T_{c\,II} \quad , \qquad (57)$$

There are five different phases of metal oxide related to the presence or the absence of perfect parallel lattice, perfect perpendicular extreme lattice, and Cooper pairs as follows.

Table 4. The Phases of Metal Oxides

| Phase/structure	perfect parallel extreme lattice for spinons	perfect perpendicular extreme lattice for phonons	Cooper pair
Insulator	no	no	no
Pseudogap	no	yes	yes
Superconductor	yes	yes	yes
non-fermi liquid	no	no	yes
normal conductor	no	no	no

.

Without doping, metal oxide is an insulator. The pseudogap phase has a certain amount of doping. With a certain amount of doping, the perfect perpendicular extreme lattice can be established with the pseudogap transition temperature, T_p, equal to $T_{c\perp}$. However, the parallel lattice is imperfect with gaps, so it is not a superconductor. The pseudogap phase can also be achieved by the increase in temperature above T_c to create gap in the parallel extreme lattice, resulting in imperfect parallel extreme lattice. Different points in the pseudogap phase represent different degrees of the imperfect parallel extreme lattice. With the optimal doping, the pseudogap phase becomes the superconductor phase below T_c. Superconductor has perfect parallel extreme lattice and perfect perpendicular extreme lattice. With excessive doping, the superconductor phase becomes the conductor phase without significant spin fluctuation and lattice vibration. In the non-fermi liquid region, the extreme lattice is imperfect by the combination of the moderate increase in temperature above T_c and the moderate increase in doping. However, non-fermi liquid phase still has Cooper pairs that do not require the presence of perfect extreme lattice. In the non-fermi liquid phase, due to the breaking of Cooper pairs with the increase in temperature, the transport properties are temperature dependent, unlike normal conductor.

In summary, for a low-temperature superconductor, extreme bosons are generated by the quantum fluctuation in lattice vibration by the absorption and the emission of phonons between passing electrons and lattice atoms. The connection of extreme bosons results in extreme lattice and Cooper pairs. For a high-temperature superconductor, extreme bosons are generated by the quantum fluctuation in spin fluctuation and lattice vibration by the absorption and the emission of spinons and phonons, respectively. The extreme lattice consists of the parallel extreme bonds and the perpendicular extreme bonds. Because many extreme bosons are generated from many spin fluctuations, T_c is high.

The extreme boson can also explain the fractional quantum Hall effect (FQHE) [61] [62]. In the FQHE, electrons travel on a two-dimensional plane. In two-dimensional systems, the electrons in the direction of the Hall effect are completely separate, so the extreme bond cannot be formed between the electrons. However, an individual electron can have n extreme bosons from the quantum fluctuation of the

magnetic flux at a very low temperature, resulting in extreme atom that consists of an electron and n extreme bosons with n extreme boson force fields.

Extreme boson force field consists of a core vacuum surrounded by only one extreme boson shell. An electron can be in $n \geq 1$ extreme boson force fields. If $n = 1$, an electron in a extreme boson force field delocalizes to the extreme boson shell, resulting in the probability distribution in both the center and the boson shell denoted as the extreme atomic orbital. (Unlike extreme boson force field, gauge boson force field can have infinitive number of orbitals.) The probability distribution factionalizes the electron into one fractional electron at the center and the 2p fractional electron in the extreme atomic orbital. Thus, the extreme atom ($n = p = 1$) has three fractional electrons, and each fractional electron has $-1/3$ charge. For $n > 1$, the multiple extreme force fields are like multiple separate bubbles with one fractional electron at the center. For $p = 1$ and $n = 3$, the total number of fractional electrons is 7, and each fractional electron has $-1/7$ charge as follows.
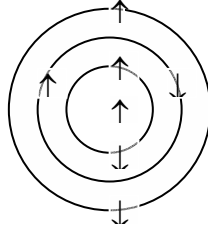
The formulas for the number of fractional electrons and fractional charge are as follows.

$$number\ of\ fractional\ electrons\ =\ 2\,pn\ +\ 1$$
$$electric\ ch\arg e\ =\ -1/\ (2\,pn\ +\ 1)$$

(58)

where n = the extreme atomic orbital number and 2p = number of fractional electrons per orbital. The wavefunction of the extreme atom is as follows.

$$\Psi_n = \Phi \sum_n \left(\prod_{j<k} (Z_j - Z_k)^{2p} \right)_n \ ,$$

(59)

where Φ is for the fractional electron at the center, $z_j = x_j - iy_j$, n = number of extreme atomic orbital, and 2p = number of fractional electrons per orbital. For the integer quantum Hall effect, $p = n = 0$. Eq. (59) is an electron in one or multiple extreme boson force fields. The probability distribution factionalizes the electrons into the k fractional electron at the center (Φ) and the 2p j fractional electrons in the extreme atomic orbital. In Eq. (59), the j fractional electron in the extreme atomic orbital takes a loop around the k fractional electron at the center. One extreme boson force field can have only one extreme atomic orbital. When the electron is in multiple n extreme boson force fields, there are n separate extreme atomic orbitals with different sizes.

This wavefunction is same as same as the wavefunction of the composite fermion, which consists of an electron and 2p flux quanta [63]. In the composite fermion, Φ is the

non-interacting electron and 2p is the number of flux quanta. The composite fermion is the bound state of an electron and 2p quantum vortices. In the same way, the extreme atom is the bound state of a fractional electron and 2pn fractional electrons in the extreme atomic orbitals. The extreme atomic orbital can be also described by the Laughlin-Jastrow factor by counting the centered fractional electron as a part of the extreme atomic orbital electrons, resulting in odd number of quasiparticles.

The extreme atoms provide the ground state for the Laudau level. Within the ground state, the extreme atom with higher n and p has higher energy and lower probability. During the generation of the Landau levels, the fractional electrons come off the extreme atomic orbitals. The most favorable way is to remove one fractional electron per extreme atomic orbital to provide more room for the other fractional electron in the same extreme atomic orbital. For n =1, one -1/3 charged electron comes off. For n = 2, two -1/5 charged electrons come off. The formula is - n / (2n+ 1) electric charge as observed: -1/3, -2/5, -3/7… [64]. The second series is the leftover of the first series: -2/3, -3/5, -4/7…

5.3.   Gravastar and Supernova

Black hole has been a standard model for the collapse of a supermassive star. Two alternates for black hole are gravastar [65] [66] and dark energy star [67]. Gravastar is a spherical void as Bose-Einstein condensate surrounded by an extremely durable form of matter. For dark energy star, the mass-energy of the nucleons under gravitational collapse can be converted to vacuum energy. The negative pressure associated with a large vacuum energy prevents the formation of singularity and results in an explosion. This paper proposes gravastar based on the stellar extreme force field in a gravastar.

Under high pressure-temperature, massless particles such as photon are converted into massive lepton pairs such as massive e+e- pairs inside the stellar extreme force field in a gravastar.   It is similar to the massive e+e- pair production from photon proposed by Rakavy, Shaviv, and Barkat [68]

$$photons \xrightarrow{\;high\;pressure-temperature\;} massive\;lepton\;pairs\;in\;stellar\;extreme\;force\;field \qquad (60)$$

The exclusion of gravity by the stellar extreme force field as in the Meissner effect prevents the gravitational collapse into singularity. The core of gravastar is the lepton pairs-stellar extreme force field as the LSC. The minimum mass of a star to have enough pressure-temperature to generate the LSC is between 24 and 40 solar masses.

Massive stars with the mass greater than 8 solar masses can undergo core collapse when nuclear fusion suddenly becomes unable to sustain the core against its own gravity. The collapse may cause violent expulsion of the outer layers of the star resulting in a supernova. The remnants of supernovae may be neutron stars or a gravastars with the LSC.

The results of the collapses of massive stars depend on their masses [69]. For the stars with masses between 8 and 25 solar masses, the remnants of supernovae are neutron stars. For the stars with masses between 24 and 40 solar masses, the remnants can be neutron stars or gravastars with the LSC depending on the metallicity. Therefore, the

minimum mass of a star to have enough pressure-temperature to generate the LSC is between 24 and 40 solar masses. For the stars with the masses between 40 and 100 solar masses, the remnants are gravastars with the LSC.

For the stars with masses between 100 and 130 solar masses, there is enough pressure and temperature to form the LSC before the collapse. The formation of the LSC with reduced volume and pressure than the original photon caused the partial collapse of the star. The result is partial ejections of parts of the outer layers of the star until its remaining core is small enough to collapse in a normal supernova with gravastars as the remnants.

For the stars between 130 and 250 solar masses, the formation of the LSC before the collapse is strong enough in terms of reduced size and pressure to cause a violent total collapse of the stars, resulting in a thermonuclear explosion with much greater brightness than the normal supernovae [70]. With more thermal energy released than the stars' gravitational binding energy, the star is completely disrupted; no gravastar or other remnant is left behind. (The outer layer outside of the LSC is high, so the collapsing energy from the high outer layer outside of the LSC is enough to destroy the LSC.)

For the stars greater than 250 solar masses, the endothermic (energy-absorbing) reaction from extremely high gravity causes the stars to continue collapse into a gravastars with the LSC without exploding due to thermonuclear reactions.

5.4   Summary

Under extreme conditions, such as the zero temperature and extremely high pressure, the extreme force fields as extreme boson force fields form. The formation of the extreme molecule (the Cooper pair) and the extreme lattice provides the mechanism for the phase transition to superconductivity, while the formation of extreme atom with electron-extreme boson provides the mechanism for the phase transition to the fractional quantum Hall effect. The formation of the stellar extreme force field in a collapsing star prevents singularity as in black hole, resulting in the formation of gravastar without singularity and with the lepton pairs-stellar extreme force field core.

6. Summary

Through the zero-energy universe and the space-object structures, the unified theory of physics is the theory of everything to explain fully cosmology, dark energy, dark matter, baryonic matter, quantum mechanics, elementary particles, force fields, galaxy formation, and unusual extreme forces. In the unified theory, different universes (zero energy, membrane, string, >4D particle, and 4D particle universes) in different developmental stages are the different expressions of the space-object structures. The unified theory is divided into five parts: (1) the space-object structures, (2) cosmology, (3) the periodic table of elementary particles, (4) the galaxy formation, and (5) the extreme force field.

(1) The unified theory is based on the space-object structures. The space structure includes attachment space and detachment space. Relating to rest mass, attachment space attaches to object permanently with zero speed. Relating to kinetic energy, detachment space detaches from the object at the speed of light. The Higgs boson mediates the transformation between these two space structures. The combination of attachment space and detachment space brings about three different space structures: miscible space, binary lattice space, and binary partition space for special relativity, quantum mechanics, and the extreme force fields, respectively. The object structure consists of 11D membrane (3_{11}), 10D string (2_{10}), variable D particle ($1_{4 \text{ to } 10}$), and empty object ($0_{4 \text{ to } 11}$). The transformation among the objects is through the dimensional oscillation that involves the oscillation between high dimensional space-time with high vacuum energy and low dimensional space-time with low vacuum energy. Our observable universe with 4D space-time has zero vacuum energy. Different universes in different developmental stages are the different expressions of the space-object structures. (2) From the zero-energy universe, our universe starts with the 11-dimensional membrane dual universe followed by the 10-dimensional string dual universe and then by the 10-dimensional particle dual universe, and ends with the asymmetrical dual universe with variable dimensional particle and 4-dimensional particles. This 4-stage process goes on in repetitive cycles. Such 4-stage cosmology accounts for the origins of the four force fields. The theoretical calculated percentages of dark energy, dark matter, and baryonic matter are 72.8. 22.7, and 4.53, respectively, in agreement with observed value. According to the calculation, dark energy started in 4.47 billion years ago in agreement with the observed 4.71 ± 0.98 billion years ago. (3) The unified theory places all elementary particles in the periodic table of elementary particles with the calculated masses in good agreement with the observed values by using only four known constants: the number of the extra spatial dimensions in the eleven-dimensional membrane, the mass of electron, the mass of Z boson, and the fine structure constant. The LHC Higgs boson is the SM Higgs boson with the hidden lepton condensate. (4) The inhomogeneous structures, such as galaxy, are derived from the incompatibility between baryonic matter and dark matter, like the inhomogeneous structure formed by the incompatibility between oil and water. Cosmic radiation allows dark matter and baryonic matter to be compatible. As the universe expanded, the decreasing density of cosmic radiation increased the incompatibility, resulting in increasing inhomogeneous structures. The five stages of the formation of inhomogeneous structures are baryonic matter, baryonic droplets, the first generation galaxies by the Big Eruption, cluster, and supercluster. The Big Eruption explains the origin of different types of galaxies. (5) Under extreme conditions, such as the zero temperature and extremely high pressure-temperature,

gauge boson force field undergoes the phase transition to form extreme force field. Extreme force field explains unusual phenomena such as superconductor, fractional quantum Hall effect, supernova, and gravastar.

Reference

[1] Berman, Marcelo Samuel "On the Zero-energy Universe". International Journal of Theoretical Physics 48 (11): 3278, 2009 arXiv:gr-qc/0605063v3.

[2] Guth, Alan H. The Inflationary Universe, Reading, Massachusetts: Perseus Books, 1997

[3] Stephen Hawking, A Brief History of Time, Bantam Dell Publishing Group, 1988, page p129,

[4] D. Chung and V. Krasnoholovets, The Cosmic Organism Theory, Scientific Inquiry 8 (2007), 165-182, http://www.iigss.net/Scientific-Inquiry/Dec07/3-krasnoholovets.pdf, arXiv: physics/0512026, http://arxiv.org/PS_cache/physics/pdf/0512/0512026v1.pdf

[5] D. Chung,, The Unified Theory of Physics, arXiv:hep-th/0201115, http://arxiv.org/ftp/hep-th/papers/0201/0201115.pdf

[6] V. Krasnoholovets, and D. Y. Chung, The Space Structure, Force Fields and Quantum Mechanics,, International Journal of Anticipatory Computing Systems (2006), ed. by D. Dubois, 191-197, http://inerton.org/Inerton_Theory_-_Papers_-_Sub-microscopic_Mechanics_files/30_Chung&Krasn_1.pdf

[7] D. Chung, D. and V. Krasnoholovets, V., The Quantum Space Phase Transitions for Particles and Force Fields, Progress in Physics 4 (2006) 74, http://www.ptep-online.com/index_files/2006/PP-06-14.PDF

[8] B. M. Diaz and P. Rowlands, American Institute of Physics Proceedings of the International Conference of Computing Anticipatory Systems (2003), ed. Daniel Dubois

[9] J. S. Bell, Physics 1 (1964), 195

[10] R. Penrose, Mathematical Physics (2000) eds: by A. Fokas, A. Grigoryan, T. Kibble & B. Zegarlinski (Imperial College, London), pp. 266-282.

[11] A. H. Guth, Phys. Rev. D 23 (1981) 347 ; A. Vilenkin, Phys. Rev. D 27 (1983) 2848; A. Linde, A. Phys Lett B175 (1986) 395

[12] J. Moffat, Int. J. Mod. Phys. D2 (1993)351 [arXiv: gr-qc/9211020]

[13] A. Albrecht and J. Magueijo, Phys.Rev. D59 (1999) 043516 [arXiv: hep-ph/9811018]

[14] J. D. Barrow, Phys. Lett. B564 (2003) 1, [arXiv: gr-qc/0211074]

[15] T. R. Mongan, General Relativity and Gravitation 33 (2001) 1415 [arXiv: gr-qc/0103021]; General Relativity and Gravitation 37 (2005) 967 [arXiv: gr-qc/0501014]

[16] J. D. Barrow, G. F. R. Ellis, R. Maartens, and C. G. Tsagas, Class Quantum Grav. 20 (2003), L155 [arXiv: gr-qc/0302094]

[17] L. Randall and R. Sundrum, Phys.Rev.Lett. 83 (1999) 4690 [arXiv: hep-th/9906064]

[18] M. Bounias and V. Krasnoholovets, The Int. J. Systems and Cybernetics 32, (2003) 1005-1020 [arXiv: physics/0301049]

[19] J. Maldacena, Adv. Theor. Math. Phys. V. 2 (1998) 231 [arXiv: hep-th/9711200]

[20] S. S. Gubser, I. R. Klebanov, and A. M. Polyakov, Phys. Lett.B v. 428 (1998) 105 [arXiv: hep-th/9802109]

[21] E. Witten, Adv. Theor. Math. Phys. V. 2 (1998) 253 [arXiv: hep-th/9802150]

[22] P. J. Steinhardt and N. Turok, Phys.Rev. D65 (2002) 126003 [arXiv: hep-th/0111098]

[23] J. Khoury, Invited talk at the 6th RESCEU Symposium, 2003, [arXiv: astro-ph/0401579]

[24] R. M. Santilli, Isodual theory of antimatter with applications to antigravity, grand unification, and cosmology" (Kluwer Academic Publishers, Boston/Dordrecht/London) 2006.

[25] T. Padmanabhan, Phys. Rept. 380 (2003) 235

[26] M. Bounias and V. Krasnoholovets, The Int. J. Systems and Cybernetics 32, no. 7/8, (2003) 945-975 [arXiv: physics/0211096]

[27] N. Jarosik et al, "Seven-Year Wilson Microwave Anisotropy Probe (WMAP) Observations: Sky Maps, Systematic Errors, and Basic Results" (PDF). nasa.gov. http://lambda.gsfc.nasa.gov/product/map/dr4/pub_papers/sevenyear/basic_results/wmap_7yr_basic_res

ults.pdf. Retrieved 2010-12-02. (see p. 39 for a table of best estimates for various cosmological parameters) arXiv:1001.4744v1 [astro-ph.CO] 2010

[28] B. Feng, X. L. Wang and X. Zhang, Phys. Lett. B607 (2005) 35.

[29] Z.K. Guo, Y.S. Piao, X. Zhang and Y.Z. Zhang, Phys. Lett. B608 (2005) 177.

[30] M. Li, B. Feng and X. Zhang, JCAP 0512 (2005) 002.

[31] Y. F. Cai, T. Qiu, Y. S. Piao, M. Li and X. Zhang, JHEP 0710, 071 (2007) [arXiv: gr-qc/07041090].

[32] Y. F. Cai, T. Qiu,, R. Brandenberger, Y. S. Piao, and X. Zhang, arXiv: hep-th/ 07112187

[33] Riess, A. G., et al. Astrophysical Journal, 607, 665-687, 2004 arXiv:astro-ph/0402512v2

[34] D. Chung, Speculations in Science and Technology 20 (1997) 259 [arXiv: hep-th/0111147]

[35] Particle data Group, (2004) $\sin^2 \theta_w = 0.2397$

[36] A.O. Barut, Phys. Rev. Lett. 42(1979) 1251; A. Gsponer and J. Hurni, arXiv: hep-ph/0201193

[37] P. Langacher, M. Luo , and A. Mann, Rev. Mod. Phys. 64 (1992) 87

[38] C.P. Singh, Phys. Rev. D24 (1981) 2481; D. B. Lichtenberg Phys. Rev. D40 (1989) 3675

[39] Particle data Group, (2004)

[40] The ATLAS Collaboration, Observation of a new particle in the search for the Standard Model Higgs boson with the ATLAS detector at the LHC, arXiv:1207.7235v1 [hep-ex] July 31. 2012, The CMS Collaboration, Observation of a new boson at a mass of 125 GeV with the CMS experiment at the LHC, arXiv:1207.7235v1 [hep-ex], July31, 2012

[41] Pier Paolo Giardino, Kristjan Kannike, Martti Raidal, Alessandro Strumia, Is the resonance at 125 GeV the Higgs boson? arXiv:1207.1347v1 [hep-ph], Karen R. Bland, for the CDF, D0 Collaborations, Search for the Higgs boson in H->γγ decays in $p\bar{p}$ collisions at 1.96 TeV, arXiv:1110.1747v1 [hep-ex]

[42] V.A. Miransky, Masaharu Tanabashi, Koichi Yamawaki, Is the t Quark Responsible for the Mass of W and Z Bosons? Mod.Phys.Lett.A4:1043,1989. Anna Hasenfratz, Peter Hasenfratz, Karl Jansen, Julius Kuti, Yue Shen, The Equivalence of the top quark condensate and the elementary Higgs field, Nuclear Physics B, Volume 365, Issue 1, 4 November 1991,

[43] S. F. King, Phys. Rev.D46, 4097, Four-family lepton mixing, 1992. S F King, Low Scale Technicolour at LEP , Phys.Lett. B314 364-370, 1993 arXiv:hep-ph/9306236v1

[44] K. Miuchi et al, Astropart. Phys. 19, 135 (2003) [arXiv: astro-ph/ 0204411]; CDMS Collaboration, Phys.Rev. D68, 082002 (2003) [arXiv: hep-ex/0306001]

[45] M. Milgrom, New Astron.Rev. 46 (2002) 741-753 [arXiv: astro-ph/0207231], astro-ph/0112069; R. H. Sanders and S. McGaugh arXiv: astro-ph/0204521

[46]D. Chung, The Evolution of Galaxies by the Incompatibility between Dark Matter and Baryonic Matter, arXiv: hep-th/0112036, http://arxiv.org/ftp/hep-th/papers/0112/0112036.pdf

[47] A. H. Guth, Phys. Rev. D 23, 347 (1981), A. D. Linde, Phys. Lett. B108 (1982) 389; A. Albrecht and P. J. Steinhardt, Phys. Rev. Lett. 48 (1982) 1220

[48] A. C. S. Readhead et al astro-ph/0402359; Rafael Rebolo et al astro-ph/0402466

[49] Valentino González et al, The Stellar Mass Density And Specific Star Formation Rate Of The Universe At Z ~ 7, ApJ 713 115, 2010, arXiv:0909.3517

[50] Mark Dijkstra and Abraham Loeb, MNRAS, 400, 1109, 2009,.arXiv:0902.2999v1 [astro-ph.CO]

[51] R. Barkana and A. Loeb, arXiv: astro-ph/0209515

[52] C. Conselice, arXiv: astro-ph/0212219

[53 B. M. Poggianti, astro-ph/0210233, S. F. Helsdon and T. J. Ponman, arXiv: astro-ph/0212047

[54] S. Leon, J. Braine, P. Duc, V. Charmandaris, and E. Brinks, astro-ph/0208494, arXiv: astro-ph/0210014

[55] M. Bonamente, M. Joy, and R. Liu, arXiv: astro-ph/0211439

[56] J. Einasto, G. Hutsi, M. Einasto, E. Saar, D. L. Tucher, V. Muller, P. Heinamaki, and S. S. Allam, arXiv: astro-ph/0212312

[57] M. J. West, astro-ph/9709289

[58] P. Coleman and A. Schofield, Nature 433 (2005) 226

[59] P. W. Anderson, P. A. Lee, M. Randeria, T. M. Rice, N. Trivedi, and F. C. Zhang Phys.: Condens. Matter 16 (2004) R755-R769, cond-mat/0311467

[60] A. Ramsak and P. Prelovsek, P. Proc. of SPIE (2005) 59320G-2, cond-mat/0506726

[61] D. C. Tsui, H. L. Störmer, and A. C. Gossard, *Phys. Rev. Lett*. 48 (1982) 1559-1562

[62] R. B. Laughlin, Phys. Rev. Lett. 50 (1983) pp 1395-1398

[63] J. K. Jain, Phys. Rev. Lett.63 (1989) pp. 199-202

[64] H. Stormer, Physica B 177 (1992) pp. 401-408.

[65] P. O. Mazurand E. Mottola, "Gravitational condensate stars: An alternative to black holes", preprint LA-UR-01-5067 (2001) [arXiv: gr-qc/0109035]

[66] P. O. Mazur and E. Mottola, Proc. Nat. Acad. Sci. 111 (2004) pp. 9545-9550 [arXiv: gr-qc/0407075]

[67] G. Chapline, Proceedings of the Texas Conference on Relativistic Astrophysics, Stanford, CA, December, 2004 [arXiv: astro-ph/0503200]

[68] Rakavy, G., & Shaviv, G. 1967, ApJ, 148, 803, Barkat, Z., Rakavy, G., & Sack, N. 1967, Phys. Rev. Lett., 18, 379

[69] Heger, A.; Fryer, C. L.; Woosley, S. E.; Langer, N.; Hartmann, D. H. "How Massive Single Stars End Their Life". The Astrophysical Journal 591: 288, 2003

[70] Gal-Yam, A.; Mazzali, P.; Ofek, E. O.; Nugent, P. E.; Kulkarni, S. R.; Kasliwal, M. M.; Quimby, R. M.; Filippenko, A. V. et al. "Supernova 2007bi as a pair-instability explosion". Nature 462 (7273): 624–627 , 2009